



Title	Study on Function of Protein Phosphatase PPM1D in Carcinogenesis and Cell Differentiation
Author(s)	小笠原, 紗里
Citation	北海道大学. 博士(理学) 甲第13669号
Issue Date	2019-03-25
DOI	10.14943/doctoral.k13669
Doc URL	<a href="http://hdl.handle.net/2115/77065">http://hdl.handle.net/2115/77065</a>
Type	theses (doctoral)
File Information	Sari_Ogasawara.pdf



[Instructions for use](#)

**Study on Function of Protein Phosphatase  
PPM1D in Carcinogenesis and  
Cell Differentiation**

(発癌および細胞分化における  
脱リン酸化酵素 PPM1D の機能に関する研究)

Laboratory of Biological Chemistry,  
Graduate School of Chemical Sciences and Engineering,  
Hokkaido University

**Sari Ogasawara**

**2019**

## Table of Contents

### Abbreviations

#### 1. General introduction

1.1. Wild-type p53-induced phosphatase 1, PPM1D	1
1.2. PPM1D aberration in tumors	7
1.3. PPM1D inhibitors	7
1.4. Functions of PPM1D in physiological processes	10
1.5. Cell differentiation and retinoic acid signaling	11
1.6. Aims of this study	14
1.7. References	16

#### 2. Development of novel PPM1D inhibitors

2.1. Abstract	29
2.2. Introduction	31
2.3. Experimental procedures	33
2.3.1. Chemicals	33
2.3.2. <i>In vitro</i> phosphatase assay	33
2.3.3. Cell viability assay	33
2.3.4. Uptake rate assay using fluorescent probe	34
2.3.5. Analysis of SL-183 metabolism	34
2.4. Results and Discussion	
2.4.1. Structure-activity relationship studies of hydrophobic groups of SL-176	
2.4.1.1. Compounds	35
2.4.1.2. Effect of analogs on <i>in vitro</i> phosphatase activity and MCF7 cell viability	35
2.4.1.3. Discussion	40
2.4.2. Structure-activity relationship studies of hydrophilic group of SL-176	
2.4.2.1. Effect of SL-175 and SL-177 on <i>in vitro</i> phosphatase activity and MCF7 cell viability	43
2.4.2.2. Effect of SL-180 and SL-183 on <i>in vitro</i> phosphatase activity	

and MCF7 cell viability	47
2.4.2.3. Effect of the amine in compound on intracellular uptake rate	47
2.4.2.4. Intracellular metabolites analysis of SL-183	52
2.4.2.5. PPM1D specificity of SL-183	52
2.4.3. Discussion	57
2.5. References	62
<b>3. Role of PPM1D in differentiation induction on NT2/D1 cells</b>	
3.1. Abstract	66
3.2. Introduction	68
3.3. Experimental procedures	70
3.3.1. Cell lines and materials	70
3.3.2. Cell manipulation	70
3.3.3. Alkaline phosphatase staining	71
3.3.4. Western blotting	71
3.3.5. Immunofluorescence	72
3.3.6. Quantitative RT-PCR	72
3.4. Results	
3.4.1. Effect of PPM1D knockdown on alkaline phosphatase activity in NT2/D1 cells	73
3.4.2. Effect of PPM1D knockdown on Oct-4 expression levels in NT2/D1 cells	73
3.4.3. RA-induced changes in gene and protein expression	73
3.4.4. Effect of SL-176 treatment on RA-induced differentiation induction	76
3.4.5. Effect of PPM1D overexpression on RA-induced differentiation induction	82
3.5. Discussion	84
3.6. References	86
<b>4. Regulation of the retinoic signal pathway via dephosphorylation of ERK-1/2</b>	
4.1. Abstract	90
4.2. Introduction	91

4.3. Experimental procedures	93
4.3.1. Cell lines and materials	93
4.3.2. Cell manipulation	93
4.3.3. Western blotting	94
4.3.4. <i>In vitro</i> phosphatase assay	94
4.4. Results	
4.4.1. Activation of MEK-ERK signaling following RA treatment in NT2/D1 cells	95
4.4.2. Dephosphorylation of ERK-1/2 <i>in vitro</i> phosphatase assay	95
4.4.3. Effect of SL-176 treatment on RA-induced ERK-1/2 activation	99
4.5. Discussion	101
4.6. References	102
<b>5. Conclusions</b>	<b>105</b>
<b>6. Acknowledgements</b>	<b>108</b>

## Abbreviations

5-ABFDA	5-aminobutylfluorescein diacetate
5-CFDA	5-carboxyfluorescein diacetate
AP	Alkaline phosphatase
ATM	Ataxia telangiectasia-mutated protein kinase
ATR	ATM and Rad3-related protein kinase
BRCA1	Breast cancer growth suppressor protein 1
Chk1/2	Checkpoint kinase
ERK-1/2	Extracellular signal-regulated kinase
FBS	Fetal bovine serum
H2AX	H2A histone family, member X
HAT	Histone acetylase
HDAC	Histone deacetylase
IR	Ionizing radiation
LIF	Leukemia inhibitory factor
MAPK	Mitogen-activated protein kinase
MCF7	Michigan cancer foundation 7
MEF	Mouse embryonic fibroblast
MSK1	Mitogen-and stress-activated kinase 1
mTOR	Mammalian target of rapamycin
NCOA	Nuclear receptor co-activators
NCOR	Nuclear receptor co-repressor
NLS	Nuclear localization sequence

Oct-4	Octamer-binding transcription factor 4
PAGE	Polyacrylamide gel electrophoresis
PAX6	Paired box 6
PBS	Phosphate buffered saline
PI3K	Phosphoinositide 3 kinase
PPIA	Peptidylprolyl isomerase A
PPM1D	Protein phosphatase 1D
RA	Retinoic acid
RAR	Retinoic acid receptor
RXR	Retinoid X receptor
SAR	Structure activity relationships
STAT	Signal transducer and activator of transcription
TGF- $\beta$	Transforming growth factor
UV	Ultraviolet

## 1. General introduction

### 1.1. Wild-type p53-induced phosphatase 1, PPM1D

Protein phosphatase 1D (PPM1D, also known as Wip1 and PP2C $\delta$ ) is a member of the PPM1 type serine/threonine phosphatases. PPM1D was originally identified as a tumor suppressor protein p53 target product, which is induced by ionizing radiation (1). PPM1D dephosphorylates and inactivates various critical factors, including activated p53, p38, mitogen-activated protein kinase (MAPK), ATM, Chk1/2, and H2AX, in response to DNA damage (2–7). PPM1D plays a critical role in modulating the cell cycle by negatively regulating the p53 pathway and DNA damage checkpoints (**Figure 1-1**).

The PPM1 family has 12 isoforms. The amino residues in the active center and the sequences in the catalytic domain are highly conserved among PPM1 family members (**Figure 1-2**). PPM1D possesses two unique loop regions in the catalytic domain (8). The proline-rich loop, or P-loop, is located at the opposite side of the active center, and the basic amino acid-rich loop, or B-loop, is located near the active center. Both loops are considered to exert specificity for substrates and regulate the phosphatase activity (**Figure 1-3**).

The *PPM1D* gene is located at 17q23.2, and *PPM1D605* comprises six exons. Our group has reported an alternative splice variant PPM1D430, which shares the catalytic domain (1-420 aa) and an additional 10 residues (**Figure 1-4, 1-5**). Real-time polymerase chain reaction analysis using a human tissue cDNA panel showed that *PPM1D605* is ubiquitously expressed in all tissues, and *PPM1D430* is especially expressed in testes and leukocytes (8).



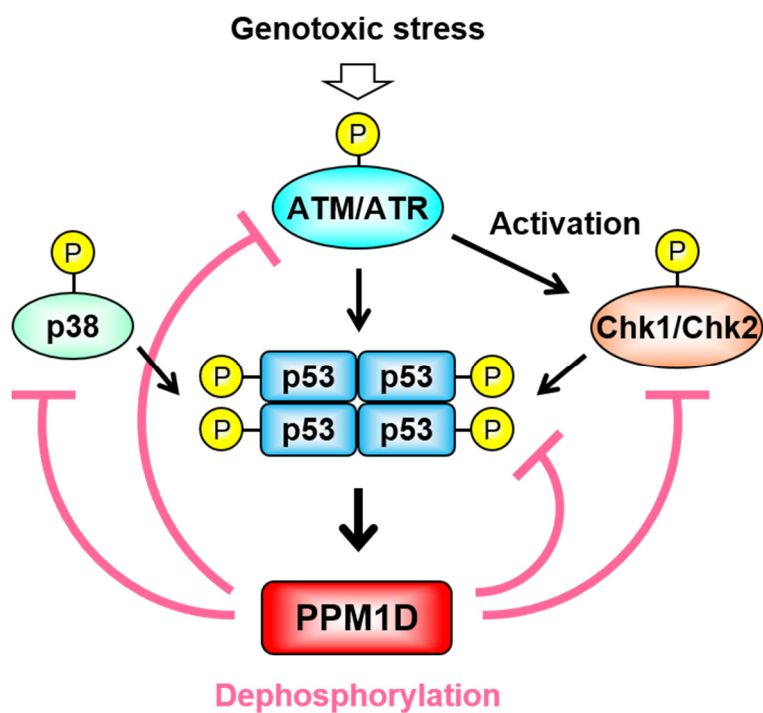


**Figure 1-1.** The main function of PPM1D phosphatase in normal cells. In response to genotoxic stress such as IR and UV, p53 is activated by DNA damage response proteins such as ATM/ATR, p38 MAPK and Chk1/2. PPM1D is transcriptionally upregulated by p53 and dephosphorylates these proteins. This negative feedback mechanism is necessary for recovery after DNA damage and some stresses.

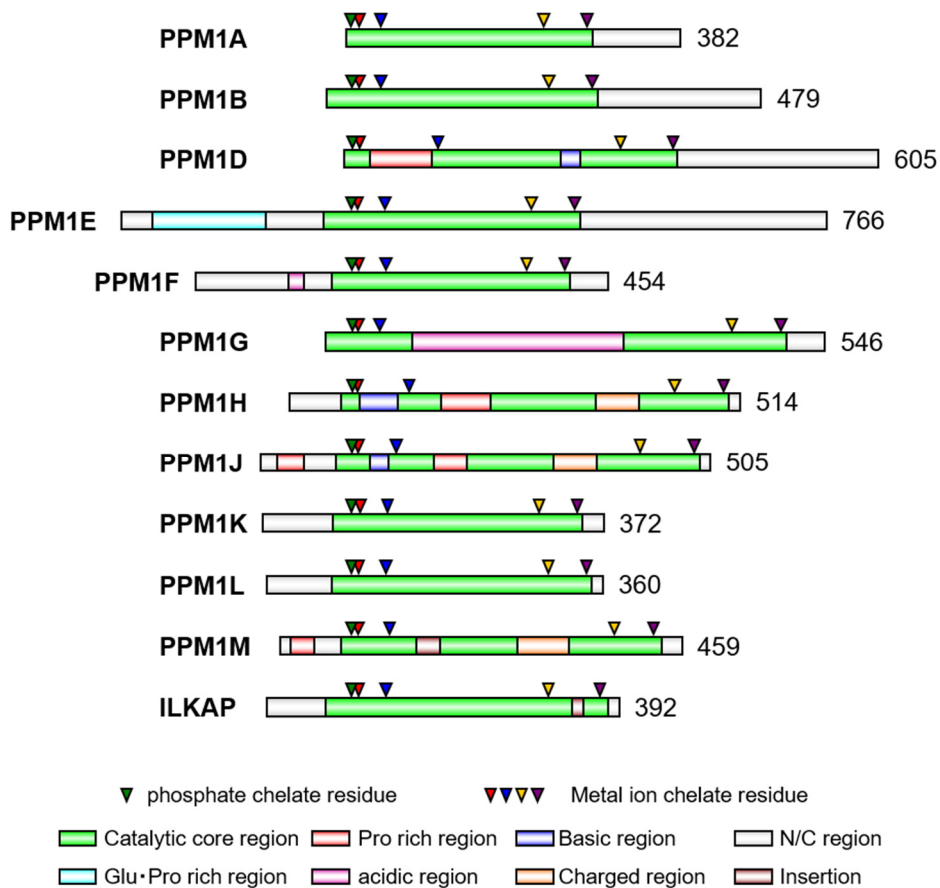


**Figure 1-2.** Domain structure of PPM1 family isoforms. Each isoform has a highly conserved catalytic domain. The inherent region of each isoform exerts the specific regulation and the substrate preference.

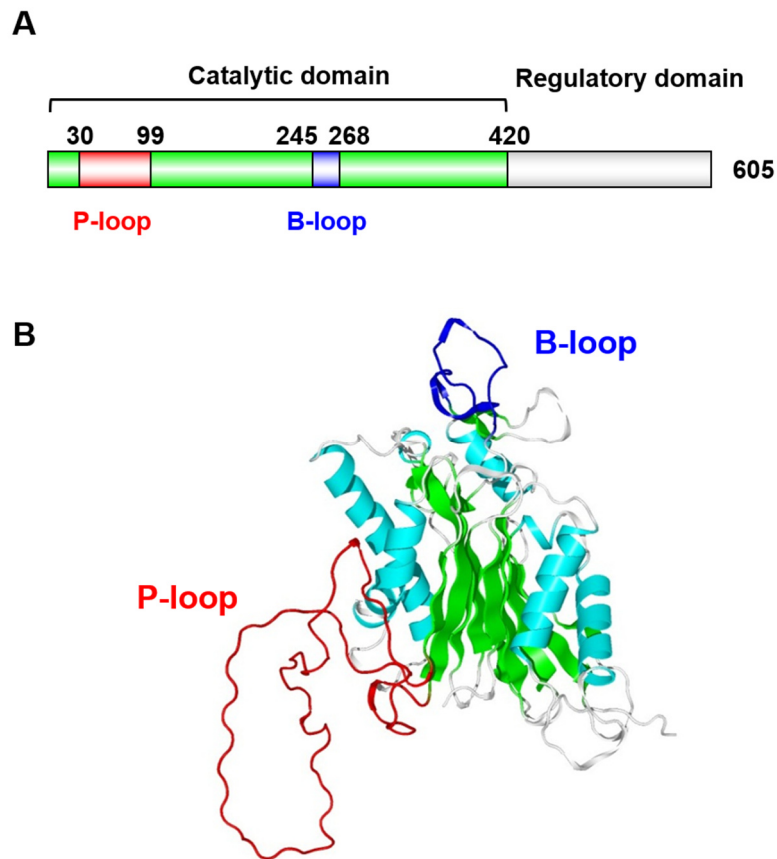


**Figure 1-3.** Schematic structure (A) and structure model of PPM1D catalytic domain (B). PPM1D consists of two domains: catalytic domain (1-420) and regulatory domain (421-605). There are two unique loop region, P-loop and B-loop, in catalytic domain. Homology modeling of PPM1D(5-385) was estimated based on the crystal structure of PPM1A, and PPM1B and PPM1K.

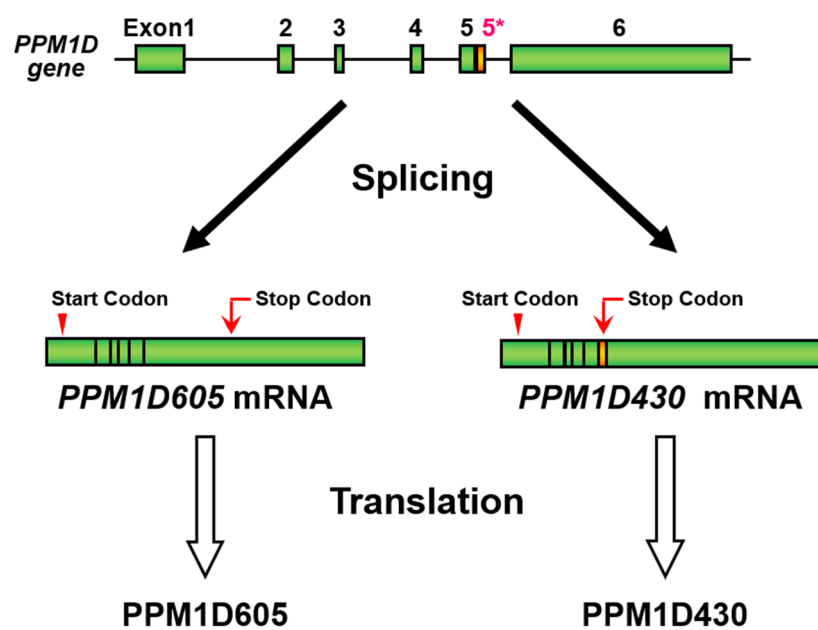
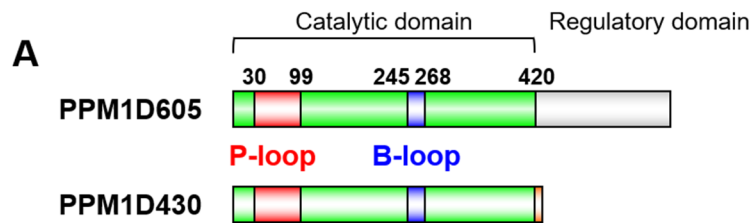


**Figure 1-4.** Schematic structures of alternative splicing of *PPM1D* gene. *PPM1D605* and *PPM1D430* mRNAs are generated by alternative splicing. The major transcript is contained six exons, exon 1, 2, 3, 4, 5 and 6, and translated to *PPM1D605*. The minor transcript is spliced with inserted exon 5' between 5 and 6, result in translation to *PPM1D430*.



**B**

*Common sequence*

1 MAGLYSLGVSVFSDQGGRRKYMEDVTQIVV**EPEPTAEKPSPRRSLSQPLP**  
**PRPSPAALPGGEVSGKGP**AVAAREARDPLPDAGASPAPSRCCRRRSSVAF  
**FA**VCDGHGGREAAQFAREHLWGF I KKQKGFTSSEPAKVCAAIRKGF LACH  
LAWKKLAEWPKTMTGLPSTSGTTASVVI IRGMKMYVAHVGD SGVVLGIQ  
DDPKDDFVRAVEVTQDHKPELPKERERIEGLGGSVMNKSGVNRV**VWKRPR**  
**LTHNGPVRRSTVIDQI**PFLAVARALGDLWSYDFFSGEFVVSPEPDTSVHT  
LDPQKHKYI I LGSDGLWNMI PPQDAI SMCQDQEEKYL MGEHGQSCAKML  
VNRALGRWRQRMLRADNTSAIVICISPEVDNQGNFTNEDELYLNLTDSPS  
YNSQETCVMTSPCSTPPVK 420

*PPM1D605(421-605)*

421 SLEEDPWPRVNSKDHI PALVRSNAFSENFLEVS AEIAREN VQGVV IPSKD  
PEPLEENCAKALTLRIHDSLNNSLPIGLVPTNSTNTVMDQKNLKMSTPGQ  
MKAQEIERTPPTNFKRTLEESNSGPI MKKHRRNGLSRSSGAQPASLPPTS  
QRKNSVKLTMRRRLRGQKKIGNPLLHQHRKTVVCV 605

*PPM1D430(421-430)*

421 **DFGFELDSRK** 430

**Figure 1-5.** Schematic domain of PPM1D variants (A) and amino acid sequence (B). PPM1D605 and PPM1D430 share the catalytic domain (1-420) which has P-loop (red) and B-loop (blue) and possess individual sequence in C-terminal.

## 1.2. PPM1D aberration in tumors

Our group demonstrated that PPM1D overexpression induces an increase in nucleolar number, which is a marker of cancer prognosis, via the CDC25C-CDK1-PLK1 pathway (9). The amplification and overexpression of PPM1D have been reported for various tumors, including breast cancer, ovarian cancer and neuroblastoma (Table 1-1) (10-35). Truncation and gain-of-function mutations have been found in cancers (24). It has been also reported that C-terminal truncation of PPM1D leads to increases in protein stability and phosphatase activity. Aberrant PPM1D has been associated with poor prognosis for patients in several cancers (23, 36). Therefore, PPM1D is considered as a potential oncogene, and it is a promising target protein in cancer therapy.

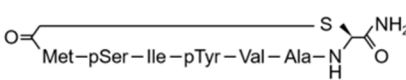
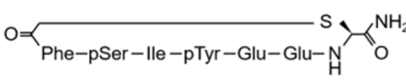
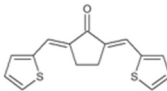
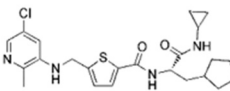
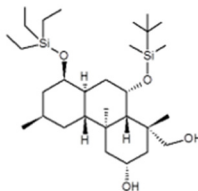
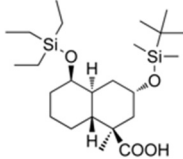
## 1.3. PPM1D inhibitors

Inhibitors that have high affinity and specificity to the PPM1D protein would generate a molecular target therapy (Table 1-2). A first specific inhibitor was designed based on the PPM1D substrate sequence. The thioether cyclic phosphopeptides c(MpSIpYVA) and c(FpSIpYDD) inhibited PPM1D phosphatase activity *in vitro* (37, 38). CCT007093 was identified by screening a small molecule library (39). Although CCT007093 was assayed for the inhibitory activity against cells with high expression of PPM1D and it was used in many studies, currently it is considered as a non-specific inhibitor. The novel orally available inhibitor GSK2830371 potently inhibited PPM1D activity *in vitro* and *in vivo* (40).

**Table 1-1.** Gene amplification and overexpression of PPM1D. In many tumors, gene amplification and overexpression of PPM1D are reported. Table 1-1 was reported by several papers and modified by our laboratory.

Tumors	Gene Amplification	mRNA/ *Protein Overexpression	Mutation	Reference
Breast cancer	37/326 (11%)	7/20 (35%)	18/6912 (0.3%)	Bulavin <i>et al.</i> [10]
	26/164 (16%)			Li <i>et al.</i> [11]
	13/117 (11%)			Rauta <i>et al.</i> [12]
	8/95 (8%)			Yu <i>et al.</i> [13]
	10/181 (6%)			Natrajan <i>et al.</i> [14]
				Lambros <i>et al.</i> [15]
Ovarian clear cell carcinoma	8/20 (40%)			Hirasawa <i>et al.</i> [17]
	9/89 (10%)			Tan <i>et al.</i> [18]
			12/1121 (1%)	Ruark <i>et al.</i> [16]
Neuroblastoma	23/25 (92%)	9/32 (28%)		Saito <i>et al.</i> [19]
Medulloblastoma	24/47 (51%)	148/168 (88%)		Mendrzyk <i>et al.</i> [20]
	6/16 (37%)	3/11 (27%)		Ehrbrecht <i>et al.</i> [21]
	7/11 (64%)	16/33 (48%)		Castellino <i>et al.</i> [22]
Gliomas		45/81 (55%)		Liang <i>et al.</i> [23]
			4/14 (29%)	Zhang <i>et al.</i> [24]
Lung cancer		52/75 (69%)		Fu <i>et al.</i> [25]
			5/543 (1%)	Zajkowicz <i>et al.</i> [26]
Colorectal cancer		252/368 (68%)		Peng <i>et al.</i> [27]
		*102/120 (85%)		Li <i>et al.</i> [28]
			4/304 (1%)	Kleiblova <i>et al.</i> [29]
Hepatocellular cancer		*48/81 (59%)		Xu <i>et al.</i> [30]
		56/86 (65%)		Li <i>et al.</i> [31]
Kidney cancer		*53/78 (68%)		Sun <i>et al.</i> [32]
Pharyngeal cancer		58/85 (69%)		Sun <i>et al.</i> [33]
Thyroid cancer			5/402 (1%)	Agrawal <i>et al.</i> [34]
Prostate cancer		3/3 (100%)		Jiao <i>et al.</i> [35]
Pancreatic cancer	8/13 (11%)	3/11 (27%)		Ehrbrecht <i>et al.</i> [21]

**Table 1-2.** List of representative PPM1D inhibitors. Structure and inhibitory activity toward PPM1D enzyme were shown.

compound	structure	IC <sub>50</sub>
<b>cyclic peptide</b>		3.7 μM * [16]
<b>cyclic peptide</b>		0.1 μM * [17]
<b>AP4-3E-A</b>	Ac-VEPPL(AP4)QEEEEELW-NH <sub>2</sub>	7.8 μM ** [11]
<b>CCT007093</b>		8.4 μM *** [18]
<b>GSK2830371</b>		294 nM ** [19]
<b>SPI-001</b>		0.48 μM ** [29]
<b>SL-176</b>		110 nM ** [30]

*in vitro* phosphatase assay; Substrates

\*; p38(pT180, pY182) peptide, \*\*; p53(pS15) peptide, \*\*\*; full length recombinant p38



We have developed a PPM1D inhibitor, SPI-001 (41), which potently inhibited phosphatase activity *in vitro*. SPI-001 also suppressed cell proliferation in a PPM1D-overexpressing human breast cancer cell line. Based on SPI-001 and a structure-activity relationship analysis, we have found a novel inhibitor, SL-176 (42). The molecular weight of SL-176 was reduced, and its inhibitory effect on cell viability was enhanced. Although SL-176 is used as a powerful tool for studying PPM1D *in vitro*, it is also of interest to optimize SL-176 and improve its inhibitory activity, specificity, and bioavailability.

#### **1.4. Functions of PPM1D in physiological processes**

Several studies have revealed the physiological functions of PPM1D such as regulation of cell senescence, autophagy, neurogenesis, spermatogenesis, immune response, maintenance of stem cells, and functional maturation of hematopoietic cells (43–49). In mesenchymal, neural, and hematopoietic stem cells, PPM1D maintains stemness through suppression of the p53 pathway, and PPM1D deficiency induces cell differentiation, cell death, and senescence (47–49). Recent evidence has supported the idea that PPM1D is a candidate gene for intellectual disability (50). Excess stem cell death was reported in *Ppm1d* knockout mice testes. Moreover, *Ppm1d*-deficient germ cells have a condensed chromatin structure, indicating the formation of a heterochromatin structure. PPM1D also directly suppresses ATM-BRCA1-dependent DNA methylation and heterochromatin formation (51).

## 1.5. Cell differentiation and retinoic acid signaling

Cell differentiation is an important process that generates multiple specialized cell lineages from unspecialized cells in response to appropriate stimuli (**Figure 1-6**). This phenomenon is mainly controlled by transcriptional factors under intrinsic and extrinsic signals, as well as the epigenetic status of cells and the microenvironment (52, 53). Many intracellular signaling pathways, such as LIF/STAT, TGF- $\beta$ , WNT/ $\beta$ -catenin, Notch, Hedgehog, and retinoic acid (RA) pathways, are known as regulators of both pluripotency and differentiation (54–57). Studying developmental cell biology will not only further our understanding of cell development and differentiation, but also may contribute to the development of therapeutic strategies for diseases caused by dysregulation of cell differentiation (58–60).

RA, the active metabolite of vitamin A, plays key roles in various biological processes, such as embryonic development and cell differentiation. RA is also a promising agent for cancer therapy (61, 62). RA binds to a nuclear RA receptor (RAR) that comprises three subtypes ( $\alpha$ ,  $\beta$  and  $\gamma$ ). RARs form a heterodimer complex with the retinoid X receptor (RXR). According to the classical model, the RAR-RXR complex binds to a RA response element in RA target genes. A ligand-dependent conformational change of RAR upon binding and the coregulator exchange occur, resulting in the activation of transcription (**Figure 1-7**) (63). Several studies have demonstrated non-genomic effects of RA on functions that activate the MAPK pathways in several cell lines (64–69). RA rapidly and transiently induces the activation of MAPKs, and they then translocate to the nucleus, where they phosphorylate several proteins. This process would

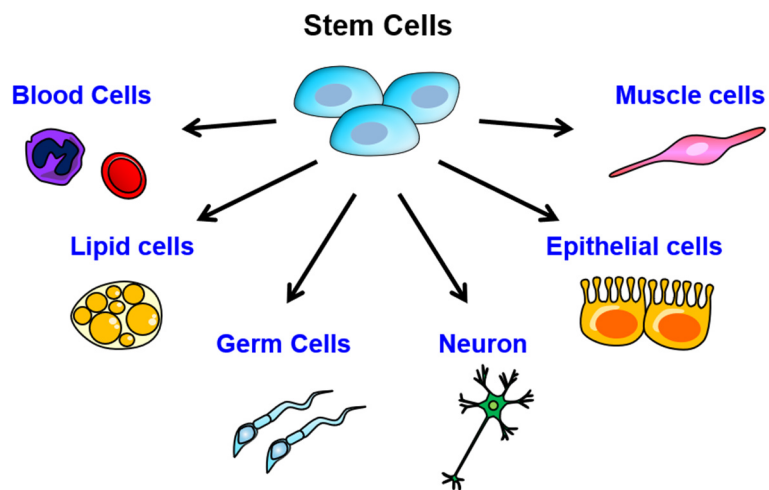


**Figure 1-6.** Scheme of stem cell differentiation. Stem cells can differentiate into multiple cell types of human tissue.

### RA-mediated gene activation

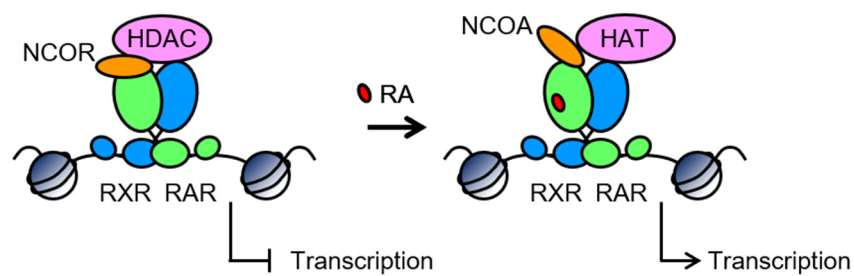


**Figure 1-7.** The canonical model of regulation of RA-mediated gene activation by RAR-RXR heterodimers. RAR and RXR form heterodimer and bound to RA response elements. In the absence of RA, co-repressors such as nuclear receptor co-repressor (NCOR) and histone deacetylase (HDAC) bind to RAR. In presence of RA, co-repressors are released and co-activators such as nuclear receptor co-activator (NCOA) and histone acetylase (HAT) are recruited. This complex activates transcription of target genes.

facilitate the exchange of coregulators and gene expression (**Figure 1-8**).

### **1.6. Aims of this study**

It has been shown that PPM1D maintains stemness, as described above. However, the precise mechanism for regulating cell stemness and its function in differentiation induction signaling still remain obscure. To understand the function of PPM1D in cell differentiation, a biochemical approach using inhibitors is important. It is also essential to clarify the identity of PPM1D target proteins and the control mechanism in the differentiation induction process. In this study, I (1) developed PPM1D inhibitors and (2) elucidate the function of PPM1D in RA differentiation induction in the human embryonic carcinoma cell line NT2/D1.

### RA-mediated MAPKs activation

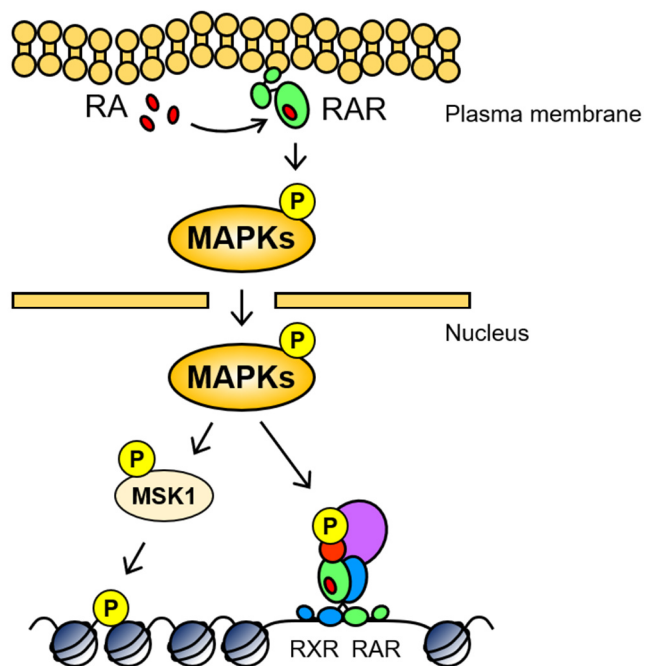


**Figure 1-8.** The non-canonical model of RA-mediated activation of kinase cascades. RA rapidly and transiently several kinase cascades. Activated MAPKs phosphorylate downstream proteins such as MSK1 and co-factors.

## 1.7. References

1. Fiscella, M., Zhang, H., Fan, S., Sakaguchi, K., Shen, S., Mercer, W. E., Vande Woude, G. F., O'Connor, P. M., and Appella, E. (1997) Wip1, a novel human protein phosphatase that is induced in response to ionizing radiation in a p53-dependent manner. *Proc. Natl. Acad. Sci. U. S. A.* **94**, 6048–53
2. Lu, X., Nannenga, B., and Donehower, L. A. (2005) PPM1D dephosphorylates Chk1 and p53 and abrogates cell cycle checkpoints. *Genes Dev.* **19**, 1162–1174
3. Takekawa, M., Adachi, M., Nakahata, A., Nakayama, I., Itoh, F., Tsukuda, H., and Imai, K. (2000) p53-inducible Wip1 phosphatase mediates a negative feedback regulation of p38 MAPK-p53 signaling in response to UV radiation. *EMBO J.* **19**, 6517–6526
4. Shreeram, S., Demidov, O. N., Hee, W. K., Yamaguchi, H., Onishi, N., Kek, C., Timofeev, O. N., Dudgeon, C., Fornace, A. J., Anderson, C. W., Minami, Y., Appella, E., and Bulavin, D. V. (2006) Wip1 Phosphatase Modulates ATM-Dependent Signaling Pathways. *Mol. Cell.* **23**, 757–764
5. Fujimoto, H., Onishi, N., Kato, N., Takekawa, M., Xu, X. Z., Kosugi, A., Kondo, T., Imamura, M., Oishi, I., Yoda, A., and Minami, Y. (2006) Regulation of the antioncogenic Chk2 kinase by the oncogenic Wip1 phosphatase. *Cell Death Differ.* **13**, 1170–1180
6. Moon, S. H., Nguyen, T. A., Darlington, Y., Lu, X., and Donehower, L. A. (2010) Dephosphorylation of  $\gamma$ H2AX by WIP1: An important homeostatic regulatory event in DNA repair and cell cycle control. *Cell Cycle.* **9**, 2092–2096

7. Cha, H., Lowe, J. M., Li, H., Lee, J. S., Belova, G. I., Bulavin, D. V., and Fornace, A. J. (2010) Wip1 directly dephosphorylates  $\gamma$ -H2AX and attenuates the DNA damage response. *Cancer Res.* **70**, 4112–4122
8. Chuman, Y., Kurihashi, W., Mizukami, Y., Nashimoto, T., Yagi, H., and Sakaguchi, K. (2009) PPM1D430, a novel alternative splicing variant of the human PPM1D, can dephosphorylate p53 and exhibits specific tissue expression. *J. Biochem.* **145**, 1–12
9. Kozakai, Y., Kamada, R., Furuta, J., Kiyota, Y., Chuman, Y., and Sakaguchi, K. (2016) PPM1D controls nucleolar formation by up-regulating phosphorylation of nucleophosmin. *Sci. Rep.* **6**, 1–11
10. Bulavin, D. V., Demidov, O. N., Saito, S., Kauraniemi, P., Phillips, C., Amundson, S. A., Ambrosino, C., Sauter, G., Nebreda, A. R., Anderson, C. W., Kallioniemi, A., Fornace, A. J., and Appella, E. (2002) Amplification of PPM1D in human tumors abrogates p53 tumor-suppressor activity. *Nat. Genet.* **31**, 210–215
11. Li, J., Yang, Y., Peng, Y., Austin, R. J., Van Eyndhoven, W. G., Nguyen, K. C. Q., Gabriele, T., McCurrach, M. E., Marks, J. R., Hoey, T., Lowe, S. W., and Powers, S. (2002) Oncogenic properties of PPM1D located within a breast cancer amplification epicenter at 17q23. *Nat. Genet.* **31**, 133–134
12. Rauta, J., Alarmo, E. L., Kauraniemi, P., Karhu, R., Kuukasjärvi, T., and Kallioniemi, A. (2006) The serine-threonine protein phosphatase PPM1D is



frequently activated through amplification in aggressive primary breast tumours.

*Breast Cancer Res. Treat.* **95**, 257–263

13. Yu, E., Ahn, Y. S., Jang, S. J., Kim, M. J., Yoon, H. S., Gong, G., and Choi, J. (2007) Overexpression of the wip1 gene abrogates the p38 MAPK/p53/Wip1 pathway and silences p16 expression in human breast cancers. *Breast Cancer Res. Treat.* **101**, 269–278
14. Natrajan, R., Lambros, M. B., Rodriguez-Pinilla, S. M., Moreno-Bueno, G., Tan, D. S. P., Marchio, C., Vatcheva, R., Rayter, S., Mahler-Araujo, B., Fulford, L. G., Hungermann, D., Mackay, A., Grigoriadis, A., Fenwick, K., Tamber, N., Hardisson, D., Tutt, A., Palacios, J., Lord, C. J., Buerger, H., Ashworth, A., and Reis-Filho, J. S. (2009) Tiling Path Genomic Profiling of Grade 3 Invasive Ductal Breast Cancers. *Clin. Cancer Res.* **15**, 2711–2722
15. Lambros, M. B., Natrajan, R., Geyer, F. C., Lopez-Garcia, M. A., Dedes, K. J., Savage, K., Lacroix-Triki, M., Jones, R. L., Lord, C. J., Linardopoulos, S., Ashworth, A., and Reis-Filho, J. S. (2010) PPM1D gene amplification and overexpression in breast cancer: A qRT-PCR and chromogenic in situ hybridization study. *Mod. Pathol.* **23**, 1334–1345
16. Ruark, E., Snape, K., Humburg, P., Loveday, C., Bajrami, I., Brough, R., Rodrigues, D. N., Renwick, A., Seal, S., Ramsay, E., Duarte, S. D. V., Rivas, M. A., Warren-Perry, M., Zachariou, A., Campion-Flora, A., Hanks, S., Murray, A., Pour, N. A., Douglas, J., Gregory, L., Rimmer, A., Walker, N. M., Yang, T. P., Adlard, J. W., Barwell, J., Berg, J., Brady, A. F., and Rahman, N. *et al.* (2013)

- Mosaic PPM1D mutations are associated with predisposition to breast and ovarian cancer. *Nature*. **493**, 406–410
17. Hirasawa, A., Saito-Ohara, F., Inoue, J., Aoki, D., Susumu, N., Yokoyama, T., Nozawa, S., Inazawa, J., and Imoto, I. (2003) Association of 17q21-q24 gain in ovarian clear cell adenocarcinomas with poor prognosis and identification of PPM1D and APPBP2 as likely amplification targets. *Clin. Cancer Res.* **9**, 1995–2004
  18. Tan, D. S. P., Lambros, M. B. K., Rayter, S., Natrajan, R., Vatcheva, R., Gao, Q., Marchio, C., Geyer, F. C., Savage, K., Parry, S., Fenwick, K., Tamber, N., Mackay, A., Dexter, T., Jameson, C., McCluggage, W. G., Williams, A., Graham, A., Faratian, D., El-Bahrawy, M., Paige, A. J., Gabra, H., Gore, M. E., Zvelebil, M., Lord, C. J., Kaye, S. B., Ashworth, A., and Reis-Filho, J. S. (2009) PPM1D Is a Potential Therapeutic Target in Ovarian Clear Cell Carcinomas. *Clin. Cancer Res.* **15**, 2269–2280
  19. Saito-Ohara, F., Imoto, I., Inoue, J., Hosoi, H., Nakagawara, A., Sugimoto, T., and Inazawa, J. (2003) PPM1D is a potential target for 17q gain in neuroblastoma. *Cancer Res.* **63**, 1876–1883
  20. Mendrzyk, F., Radlwimmer, B., Joos, S., Kokocinski, F., Benner, A., Stange, D. E., Neben, K., Fiegler, H., Carter, N. P., Reifenberger, G., Korshunov, A., and Lichter, P. (2005) Genomic and protein expression profiling identifies CDK6 as novel independent prognostic marker in medulloblastoma. *J. Clin. Oncol.* **23**, 8853–8862

21. Ehrbrecht, A., Müller, U., Wolter, M., Hoischen, A., Koch, A., Radlwimmer, B., Actor, B., Mincheva, A., Pietsch, T., Lichter, P., Reifenberger, G., and Weber, R. G. (2006) Comprehensive genomic analysis of desmoplastic medulloblastomas: Identification of novel amplified genes and separate evaluation of the different histological components. *J. Pathol.* **208**, 554–563
22. Castellino, R. C., De Bortoli, M., Lu, X., Moon, S. H., Nguyen, T. A., Shepard, M. A., Rao, P. H., Donehower, L. A., and Kim, J. Y. H. (2008) Medulloblastomas overexpress the p53-inactivating oncogene WIP1/PPM1D. *J. Neurooncol.* **86**, 245–256
23. Liang, C., Guo, E., Lu, S., Wang, S., Kang, C., Chang, L., Liu, L., Zhang, G., Wu, Z., and Zhao, Z. (2012) Over-expression of Wild-type p53-induced phosphatase 1 confers poor prognosis of patients with gliomas. *Brain Res.* **1444**, 65–75
24. Zhang, L., Chen, L. H., Wan, H., Yang, R., Wang, Z., Feng, J., Yang, S., Jones, S., Wang, S., Zhou, W., Zhu, H., Killela, P. J., Zhang, J., Wu, Z., Li, G., Hao, S., Wang, Y., Webb, J. B., Friedman, H. S., Friedman, A. H., McLendon, R. E., He, Y., Reitman, Z. J., Bigner, D. D., and Yan, H. (2014) Exome sequencing identifies somatic gain-of-function PPM1D mutations in brainstem gliomas. *Nat. Genet.* **46**, 726–730
25. Fu, Z., Sun, G., and Gu, T. (2014) Proto-oncogene Wip1, a member of a new family of proliferative genes in NSCLC and its clinical significance. *Tumor Biol.* **35**, 2975–2981

26. Zajkowicz, A., Butkiewicz, D., Drosik, A., Giglok, M., Suwiński, R., and Rusin, M. (2015) Truncating mutations of PPM1D are found in blood DNA samples of lung cancer patients. *Br. J. Cancer*. **112**, 1114–1120
27. Peng, T. S., He, Y. H., Nie, T., Hu, X. D., Lu, H. Y., Yi, J., Shuai, Y. F., and Luo, M. (2014) PPM1D is a prognostic marker and therapeutic target in colorectal cancer. *Exp. Ther. Med.* **8**, 430–434
28. Li, Z.-T., Zhang, L., Gao, X.-Z., Jiang, X.-H., and Sun, L.-Q. (2013) Expression and Significance of the Wip1 Proto-oncogene in Colorectal Cancer. *Asian Pacific J. Cancer Prev.* **14**, 1975–1979
29. Kleiblova, P., Shaltiel, I. A., Benada, J., Ševčík, J., Pecháčková, S., Pohlreich, P., Voest, E. E., Dunder, P., Bartek, J., Kleibl, Z., Medema, R. H., and Macurek, L. (2013) Gain-of-function mutations of PPM1D/Wip1 impair the p53-dependent G1 checkpoint. *J. Cell Biol.* **201**, 511–521
30. Xu, Z., Cao, C., Xia, H., Shi, S., Hong, L., Wei, X., Gu, D., Bian, J., Liu, Z., Huang, W., Zhang, Y., He, S., Lee, N. P. Y., and Chen, J. (2016) Protein phosphatase magnesium-dependent 1 $\delta$  is a novel tumor marker and target in hepatocellular carcinoma. *Front. Med.* **10**, 52–60
31. Li, G. B., Zhang, X. L., Yuan, L., Jiao, Q. Q., Liu, D. J., and Liu, J. (2013) Protein Phosphatase Magnesium-Dependent 1 $\delta$  (PPM1D) mRNA Expression Is a Prognosis Marker for Hepatocellular Carcinoma. *PLoS One*.  
10.1371/journal.pone.0060775

32. Sun, G. G., Wang, Y. D., Liu, Q., and Hu, W. N. (2015) Expression of Wip1 in Kidney Carcinoma and its Correlation with Tumor Metastasis and Clinical Significance. *Pathol. Oncol. Res.* **21**, 219–224
33. Sun, G. G., Zhang, J., Ma, X. B., Wang, Y. D., Cheng, Y. J., and Hu, W. N. (2015) Overexpression of Wild-Type p53-Induced Phosphatase 1 Confers Poor Prognosis of Patients with Nasopharyngeal Carcinoma. *Pathol. Oncol. Res.* **21**, 283–291
34. Agrawal, N., Akbani, R., Aksoy, B. A., Ally, A., Arachchi, H., Asa, S. L., Auman, J. T., Balasundaram, M., Balu, S., Baylin, S. B., Behera, M., Bernard, B., Beroukhi, R., Bishop, J. A., Black, A. D., Bodenheimer, T., Boice, L., Bootwalla, M. S., Bowen, J., Bowlby, R., Bristow, C. A., Brookens, R., Brooks, D., Bryant, R., Buda, E., Butterfield, Y. S. N., Carling, T. and Zou, L. *et al.* (2014) Integrated Genomic Characterization of Papillary Thyroid Carcinoma. *Cell.* **159**, 676–690
35. Jiao, L., Shen, D., Liu, G., Jia, J., Geng, J., Wang, H., and Sun, Y. (2014) PPM1D as a novel biomarker for prostate cancer after radical prostatectomy. *Anticancer Res.* **34**, 2919–2926
36. Yang, H., Gao, X.-Y., Li, P., and Jiang, T.-S. (2015) PPM1D overexpression predicts poor prognosis in non-small cell lung cancer. *Tumor Biol.* **36**, 2179–2184

37. Yamaguchi, H., Durell, S. R., Feng, H., Bai, Y., Anderson, C. W., and Appella, E. (2006) Development of a substrate-based cyclic phosphopeptide inhibitor of protein phosphatase 2C $\delta$ , Wip1. *Biochemistry*. **45**, 13193–13202
38. Hayashi, R., Tanoue, K., Durell, S. R., Chatterjee, D. K., Jenkins, L. M. M., Appella, D. H., and Appella, E. (2011) Optimization of a cyclic peptide inhibitor of ser/thr phosphatase PPM1D (Wip1). *Biochemistry*. **50**, 4537–4549
39. Rayter, S., Elliott, R., Travers, J., Rowlands, M. G., Richardson, T. B., Boxall, K., Jones, K., Linardopoulos, S., Workman, P., Aherne, W., Lord, C. J., and Ashworth, A. (2008) A chemical inhibitor of PPM1D that selectively kills cells overexpressing PPM1D. *Oncogene*. **27**, 1036–1044
40. Gilmartin, A. G., Faitg, T. H., Richter, M., Groy, A., Seefeld, M. A., Darcy, M. G., Peng, X., Federowicz, K., Yang, J., Zhang, S. Y., Minthorn, E., Jaworski, J. P., Schaber, M., Martens, S., McNulty, D. E., Sinnamon, R. H., Zhang, H., Kirkpatrick, R. B., Nevins, N., Cui, G., Pietrak, B., Diaz, E., Jones, A., Brandt, M., Schwartz, B., Heerding, D. A., and Kumar, R. (2014) Allosteric Wip1 phosphatase inhibition through flap-subdomain interaction. *Nat. Chem. Biol.* **10**, 181–187
41. Yagi, H., Chuman, Y., Kozakai, Y., Imagawa, T., Takahashi, Y., Yoshimura, F., Tanino, K., and Sakaguchi, K. (2012) A small molecule inhibitor of p53-inducible protein phosphatase PPM1D. *Bioorganic Med. Chem. Lett.* **22**, 729–732

42. Ogasawara, S., Kiyota, Y., Chuman, Y., Kowata, A., Yoshimura, F., Tanino, K., Kamada, R., and Sakaguchi, K. (2015) Novel inhibitors targeting PPM1D phosphatase potently suppress cancer cell proliferation. *Bioorganic Med. Chem.* **23**, 6246–6249
43. Sakai, H., Fujigaki, H., Mazur, S. J., and Appella, E. (2014) Wild-type p53-induced phosphatase 1 (Wip1) forestalls cellular premature senescence at physiological oxygen levels by regulating DNA damage response signaling during DNA replication. *Cell Cycle*. **13**, 1015–1029
44. Le Guezennec, X., Brichkina, A., Huang, Y. F., Kostromina, E., Han, W., and Bulavin, D. V. (2012) Wip1-dependent regulation of autophagy, obesity, and atherosclerosis. *Cell Metab.* **16**, 68–80
45. Zhu, Y., Demidov, O. N., Goh, A. M., Virshup, D. M., Lane, D. P., and Bulavin, D. V. (2014) Phosphatase WIP1 regulates adult neurogenesis and WNT signaling during aging. *J. Clin. Invest.* **124**, 3263–3273
46. Choi, J., Nannenga, B., Demidov, O. N., Dmitry, V., Cooney, A., Brayton, C., Zhang, Y., Mbawuike, I. N., Bradley, A., Appella, E., Donehower, L. a, and Bulavin, D. V (2002) Mice Deficient for the Wild-Type p53-Induced Phosphatase Gene (Wip1) Exhibit Defects in Reproductive Organs, Immune Function, and Cell Cycle Control. *Mol. Cell. Biol.* **22**, 1094–1105
47. Lee, J. S., Lee, M. O., Moon, B. H., Shim, S. H., Fornace, A. J., and Cha, H. J. (2009) Senescent growth arrest in mesenchymal stem cells is bypassed by Wip1-

- mediated downregulation of intrinsic stress signaling pathways. *Stem Cells*. **27**, 1963–1975
48. Zhu, Y. H., Zhang, C. W., Lu, L., Demidov, O. N., Sun, L., Yang, L., Bulavin, D. V., and Xiao, Z. C. (2009) Wip1 regulates the generation of new neural cells in the adult olfactory bulb through p53-dependent cell cycle control. *Stem Cells*. **27**, 1433–1442
49. Chen, Z., Yi, W., Morita, Y., Wang, H., Cong, Y., Liu, J. P., Xiao, Z., Rudolph, K. L., Cheng, T., and Ju, Z. (2015) Wip1 deficiency impairs haematopoietic stem cell function via p53 and mTORC1 pathways. *Nat. Commun.* **6**, 1–11
50. Jansen, S., Geuer, S., Pfundt, R., Brough, R., Ghongane, P., Herkert, J. C., Marco, E. J., Willemsen, M. H., Kleefstra, T., Hannibal, M., Shieh, J. T., Lynch, S. A., Flinter, F., FitzPatrick, D. R., Gardham, A., Bernhard, B., Ragge, N., Newbury-Ecob, R., Bernier, R., Kvarnung, M., Magnusson, E. A. H., Wessels, M. W., van Slegtenhorst, M. A., Monaghan, K. G., de Vries, P., Veltman, J. A., Lord, C. J., Vissers, L. E. L. M., and de Vries, B. B. A. (2017) De Novo Truncating Mutations in the Last and Penultimate Exons of PPM1D Cause an Intellectual Disability Syndrome. *Am. J. Hum. Genet.* **100**, 650–658
51. Filipponi, D., Muller, J., Emelyanov, A., and Bulavin, D. (2013) Wip1 Controls Global Heterochromatin Silencing via ATM/BRCA1-Dependent DNA Methylation. *Cancer Cell*. **24**, 528–541



52. Guilak, F., Cohen, D. M., Estes, B. T., Gimble, J. M., Liedtke, W., and Chen, C. S. (2009) Control of Stem Cell Fate by Physical Interactions with the Extracellular Matrix. *Cell Stem Cell*. **5**, 17–26
53. Guo, M., Bao, E. L., Wagner, M., Whitsett, J. A., and Xu, Y. (2017) SLICE: Determining cell differentiation and lineage based on single cell entropy. *Nucleic Acids Res.* 10.1093/nar/gkw1278
54. Burdon, T., Smith, A., and Savatier, P. (2002) Signalling, cell cycle and pluripotency in embryonic stem cells. *Trends Cell Biol.* **12**, 432–438
55. Neuzillet, C., Tijeras-Raballand, A., Cohen, R., Cros, J., Faivre, S., Raymond, E., and De Gramont, A. (2015) Targeting the TGF $\beta$  pathway for cancer therapy. *Pharmacol. Ther.* **147**, 22–31
56. Inestrosa, N. C., and Arenas, E. (2010) Emerging roles of Wnts in the adult nervous system. *Nat. Rev. Neurosci.* **11**, 77–86
57. Takebe, N., Harris, P. J., Warren, R. Q., and Ivy, S. P. (2011) Targeting cancer stem cells by inhibiting Wnt, Notch, and Hedgehog pathways. *Nat. Rev. Clin. Oncol.* **8**, 97–106
58. Frank, N. Y., Schatton, T., and Frank, M. H. (2010) The therapeutic promise of the cancer stem cell concept. *J. Clin. Invest.* **120**, 41–50
59. Singh, S. R., Burnicka-Turek, O., Chauhan, C., and Hou, S. X. (2011) Spermatogonial stem cells, infertility and testicular cancer. *J. Cell. Mol. Med.* **15**, 468–483

60. Wang, Z., and Chen, Z. (2008) Acute promyelocytic leukemia : from highly fatal to highly curable. *Hematology*. **111**, 2505–2515
61. Clagett-Dame, M., and Knutson, D. (2011) Vitamin a in reproduction and development. *Nutrients*. **3**, 385–428
62. Maden, M. (2007) Retinoic acid in the development, regeneration and maintenance of the nervous system. *Nat. Rev. Neurosci.* **8**, 755–765
63. Cunningham, T. J., and Duester, G. (2015) Mechanisms of retinoic acid signalling and its roles in organ and limb development. *Nat. Rev. Mol. Cell Biol.* **16**, 110–123
64. Rochette-Egly, C. (2015) Retinoic acid signaling and mouse embryonic stem cell differentiation: Cross talk between genomic and non-genomic effects of RA. *Biochim. Biophys. Acta - Mol. Cell Biol. Lipids*. **1851**, 66–75
65. López-Carballo, G., Moreno, L., Masiá, S., Pérez, P., and Baretino, D. (2002) Activation of the phosphatidylinositol 3-kinase/Akt signaling pathway by retinoic acid is required for neural differentiation of SH-SY5Y human neuroblastoma cells. *J. Biol. Chem.* **277**, 25297–25304
66. Masiá, S., Alvarez, S., de Lera, A. R., and Baretino, D. (2007) Rapid, Nongenomic Actions of Retinoic Acid on Phosphatidylinositol-3-Kinase Signaling Pathway Mediated by the Retinoic Acid Receptor. *Mol. Endocrinol.* **21**, 2391–2402
67. Dey, N., De, P. K., Wang, M., Zhang, H., Dobrota, E. A., Robertson, K. A., and Durden, D. L. (2007) CSK Controls Retinoic Acid Receptor (RAR) Signaling: a

RAR-c-SRC Signaling Axis Is Required for Neuritogenic Differentiation. *Mol.*

*Cell. Biol.* **27**, 4179–4197

68. Chen, N., and Napoli, J. L. (2007) All-trans-retinoic acid stimulates translation and induces spine formation in hippocampal neurons through a membrane-associated RAR . *FASEB J.* **22**, 236–245
69. Persaud, S. D., Lin, Y. W., Wu, C. Y., Kagechika, H., and Wei, L. N. (2013) Cellular retinoic acid binding protein I mediates rapid non-canonical activation of ERK1/2 by all-trans retinoic acid. *Cell. Signal.* **25**, 19–25

## 2. Development of novel PPM1D inhibitors

### 2.1. Abstract

PPM1D phosphatase is frequently amplified and overexpressed in human tumors. It has been reported that truncation mutations in tumors increase phosphatase activity via stabilization. Thus, PPM1D is implicated as a potential oncogene, and inhibitors targeting PPM1D would be promising candidate anticancer agents. Our group previously reported that the PPM1D inhibitor SL-176 effectively prevented cancer cell viability. In this study, I conducted structure-activity relationship (SAR) studies of SL-176 to further understand and characterize the inhibitory activity mechanism of SL-176 and its analogs.

To identify the important moieties of SL-176 against PPM1D inhibition, I examined *in vitro* phosphatase assay and MCF7 cell viability assay against a series of substituted compounds of two hydrophobic moieties. Replacement of two hydrophobic moieties with hydrogen or other less bulky groups substantially decreased the inhibitory activity. Substitution to a planar bulky molecule moderately decreased inhibitory activity. These results suggested that the presence of a hydrophobic group is required to inhibit PPM1D phosphatase activity and decrease cell viability and that the sterically demanding groups with high lipophilicity are more suitable for inhibition.

Next, to examine the effect of carboxylic acid on SL-176, a series of compounds with substituted hydrophilic groups was tested. The amine form, SL-177, had a lower inhibitory activity than the primary alcohol form SL-175 in *in vitro* phosphatase assay, while SL-177 suppressed MCF7 cell viability more strongly than SL-175. Next, I

designed new compounds that have an amino alkyl-ester band, namely SL-180 and SL-183. Both compounds showed modest inhibitory activity toward PPM1D; in contrast, they inhibited MCF7 cell viability more potently. Moreover, I examined the intracellular uptake rate using different modified fluorescein diacetates. The amine fluorescein showed a faster incorporation rate than did the carboxylic acid fluorescein. The intracellular metabolism analysis by LC-MS/MS revealed that SL-183 was converted into SL-176 in the cells. Furthermore, I analyzed the PPM1D specificity of SL-183 and SL-176 at the cellular level. SL-183 preferentially inhibited PPM1D-overexpressed cell viability. Overall, SL-183 was effectively incorporated into the cells. SL-183 was converted to SL-176 and strongly reduced cell viability depending on the PPM1D expression level.

These results suggested that SL-176 effectively inhibited PPM1D phosphatase activity via interaction with the hydrophobic moieties and the amine-esterified the carboxylic acid of SL-176 to improve its inhibitory activity. This study provided an effective strategy for developing new PPM1D inhibitors.

## 2.2. Introduction

The wild-type p53-induced phosphatase PPM1D plays a homeostatic role by inactivating DNA damage responses following genotoxic stress (1–3). The increased PPM1D levels result in downregulation of p53 and stress response pathway, implying that PPM1D is a potential oncogene. PPM1D has been found to be amplified and overexpressed in several tumors, such as human primary breast, ovarian, and neuroblastoma tumors (4–9). Thus, PPM1D is a potential therapeutic target in tumors. It is necessary to develop a novel compound having potent and specific inhibitory activity to obtain an effective outcome.

Our laboratory has developed PPM1D inhibitors. SPI-001 was identified by screening a chemical library for PPM1D phosphatase activity (10). SPI-001 showed very strong inhibition against PPM1D with a sub-micromolar IC<sub>50</sub> value. A SAR analysis indicated that two hydrophobic moieties are responsible for the inhibitory activity of SPI-001 against PPM1D. However, SPI-001 required 33 steps in synthesis. SPI-001 also has a molecular weight over 500 and calculated distribution coefficient (ClogD) over 5.0. Generally, the rule of 5 predicts that poor absorption or permeation is likely when the molecular weight is greater than 500 and the ClogD is greater than 5 (11–13). Therefore, our group developed smaller analogs of SPI-001, including SL-176 to overcome its poor solubility and high lipophilicity (14). SL-176 has two hydrophobic moieties and a carboxyl group. SL-176 more potently suppressed MCF7 cell viability than did SPI-001, and it specifically inhibited PPM1D phosphatase activity. Treatment with SL-176 increased the phosphorylation level of p53 in cells and induced apoptosis.

In this study, I studied the SAR of SL-176 against hydrophobic and hydrophilic moieties to identify important moieties for PPM1D inhibition and to develop new compounds that have inhibition more potent than that of SL-176.

## **2.3. Experimental procedures**

### **2.3.1. Chemicals**

SL-175, SL-176, SL-177, SL-180, SL-183, SL-188, SL-189, SL-194, SL-195, SL-196, 5-carboxyfluorescein diacetate and 5-aminobutylfluorescein diacetate were obtained from Laboratory of Organic Chemistry II (Faculty of Science, Hokkaido University).

### **2.3.2. *In vitro* phosphatase assay**

PPM1D(1-420) was purified as His-Tag protein as previously described (14). All peptides were manually synthesized using the Fmoc protection strategy of solid phase peptide synthesis. Fmoc amino acids were obtained from Novabiochem. The peptide fractions were purified manually by reverse-phase HPLC using Vydac C 8 (22x 250 mm). The HPLC peaks were analyzed by MALDI-TOF-MS. Phosphatase activity assays by measuring the released free phosphate using the BIOMOL GREEN Reagent (Enzo life sciences). All assays were carried out in 50 mM Tris-HCl pH7.5, 50 mM NaCl, 30 mM MgCl<sub>2</sub>, 0.1 mM EGTA, 0.02% 2-mercaptoethanol, 0.5% DMSO with 2 nM His-PPM1D(1-420) for 6 min at 30 °C. Substrate sequence was Ac-VEPPLS(P)QETFSDLW-NH<sub>2</sub> (p53(pS15)).

### **2.3.3. Cell viability assay**

MCF7 human breast cancer cell line and H1299 human non-small-cell lung cancer cell line were obtained from ATCC (Rockville, MD). H1299(PMD-9) was established as



previous described (14).  $1 \times 10^4$  cells were plated onto 96-well flat-bottomed plates and incubated for 24 h. After 24 h, the cells were treated with a range of indicated concentration. Cell viability was measured by MTS assay in Figure 2-4 and by Burkerturk line (Erma, Japan) in Figure 2-8 and 2-10 after 3 days. Data fitting was carried out by KaleidaGraph4.0 (HUKINKS).

#### **2.3.4. Uptake rate assay using fluorescent probe**

MCF7 cells were plated onto 35 mm dish and incubated for 24 h. After 24 h, the cells were treated with 0.1  $\mu\text{M}$  5-CFDA or 5-ABFDA. Cell were observed by fluorescence microscopy (BZ-9000, KEYENCE).

#### **2.3.5. Analysis of SL-183 metabolism**

Metabolite extracts were prepared from MCF7 cells at 90% confluency in 10 cm dish using 10 ml ice-cold acetone containing 10% PBS after SL-183 treatment for 6 hours. Cell suspension was incubated O/N at room temperature. The supernatant was dried at Laboratory of Organic Chemistry I (Faculty of Science, Hokkaido University). The dried extract was reconstituted in 100  $\mu\text{l}$  acetone and ultra-sonicated, and insoluble fraction was spun down at 15,000 rpm for 5 min. Evaporative concentrated supernatant injected onto the LC-MS/MS system (Global Facility Center, Hokkaido University). Chromatography was performed on InertSustainSwift C18 (100 x 1 mm, 3  $\mu\text{m}$ ) with 10 x 1 mm guard column. FT-MS and FT-MS/MS were operated in negative ESI mode by LTQ-Orbitrap XL at scanning between 300-1,200  $m/z$ .

## 2.4. Results and Discussion

### 2.4.1. Structure-activity relationship studies of hydrophobic groups of SL-176

#### 2.4.1.1. Compounds

To identify the important moieties of SL-176 against PPM1D inhibition, I designed a series of compounds in which two hydrophobic moieties were substituted with small hydrophobic or comparable moieties (**Figure 2-1**). These compounds have a *trans* decalin framework and a carboxylic acid group.

#### 2.4.1.2. Effect of analogs on *in vitro* phosphatase activity and MCF7 cell viability

The inhibition against PPM1D phosphatase activity was measured using recombinant His-PPM1D(1-420) and a phosphorylated peptide derived from p53. SL-188, which does not have a hydrophobic group, and SL-189, which is substituted to *t*Bu, reduced its inhibitory activity by 23% and 50%, respectively, at 1  $\mu$ M (**Figure 2-2, 2-3**). The substitution of TBS with the benzyl group (SL-194) or benzoyl group (SL-195) moderately decreased inhibitory activity. The conversion of TES to TBS (SL-196) had no effect on its inhibitory activity.

Next, I evaluated the effect on cell viability in PPM1D overexpressed MCF7 cells by MTS assay. SL-188 and SL-189 had little effect on cell viability (**Figure 2-4**). SL-194 and SL-195 did not decrease the viability completely, even at high concentrations. SL-196 reduced cell viability with a potency similar to that of SL-176.

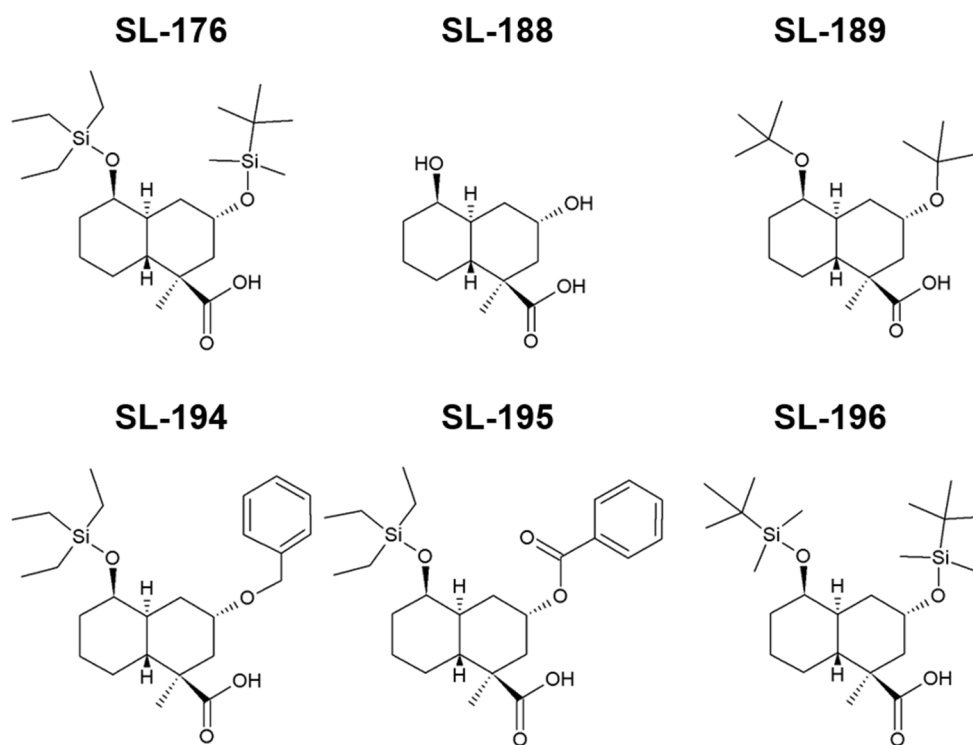


**Figure 2-1.** Structure of SL-176 and its analogs

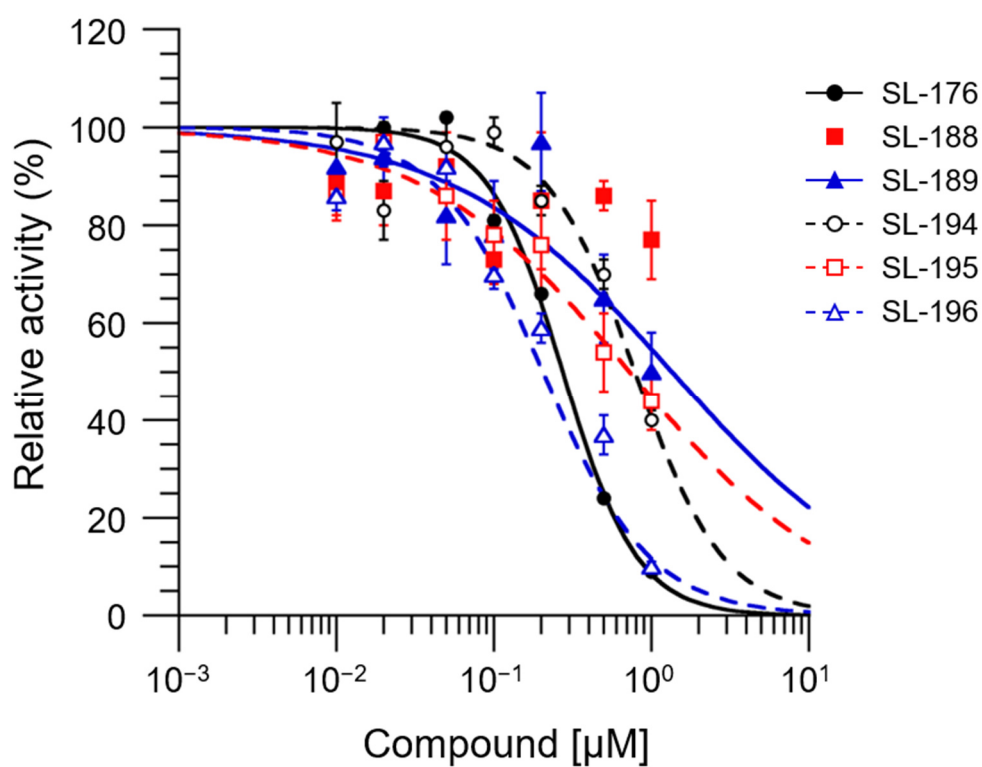


**Figure 2-2.** Inhibitory activity of SL-176 and analogs. *In vitro* phosphatase assay was carried out using His-PPM1D(1-420) enzyme and p53(10-21: pS15) peptide substrate. The black circle; SL-176, the red square; SL-188, the blue triangle; SL-189, the open black circle; SL-194, the open red square; SL-195 and the open blue triangle; SL-196. Data represent the mean  $\pm$  S.D.,  $n=3$ .

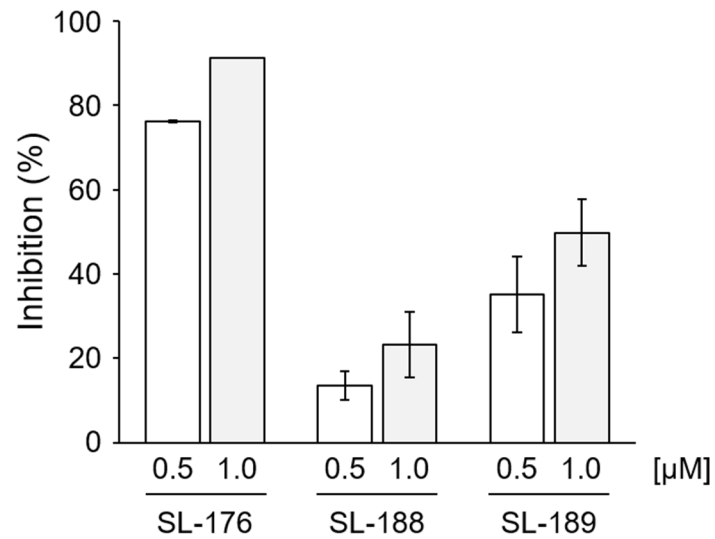


**Figure 2-3.** Inhibitory activity of SL-188 and SL-189. *In vitro* phosphatase assay was carried out using His-PPM1D(1-420) enzyme and p53(10-21: pS15) peptide substrate. Data represent the mean  $\pm$  S.D.,  $n=3$ .

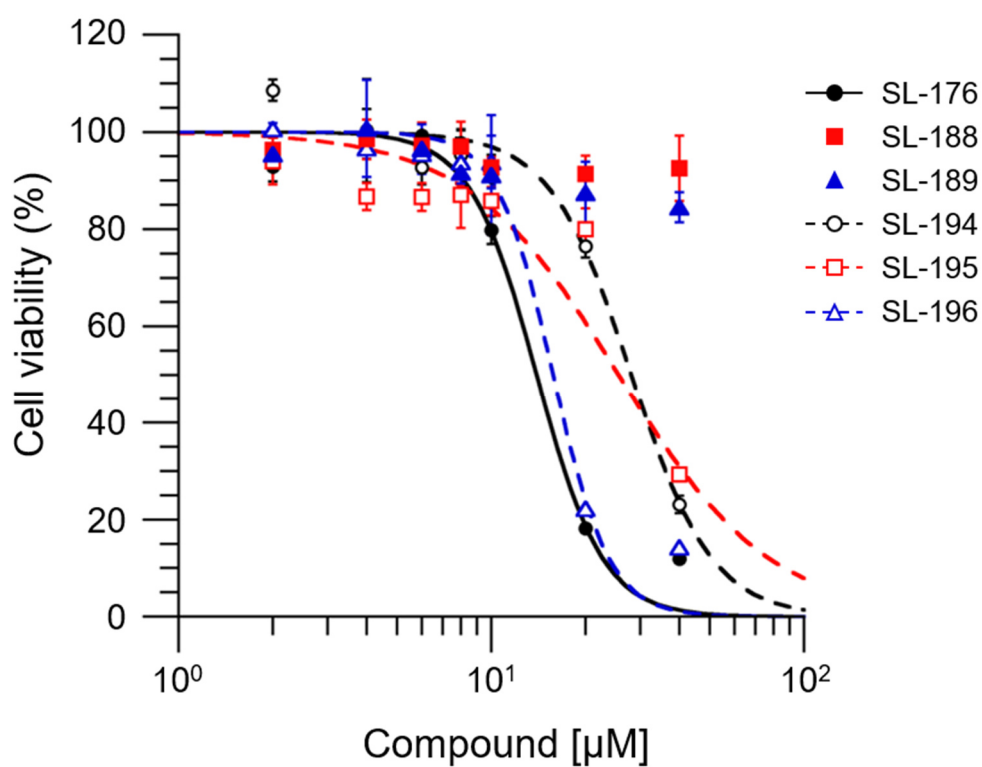


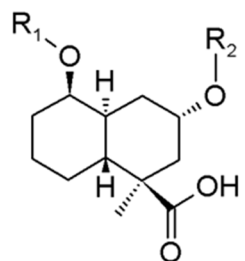
**Figure 2-4.** Cell viability of MCF7 cells under the treatment with a range of concentration of SL-175, SL-176 and SL-177. Cell viability was measured after treatment for 3 days. The black circle; SL-176, the red square; SL-188, the blue triangle; SL-189, the open black circle; SL-194, the open red square; SL-195 and the open blue triangle; SL-196. Data represent the mean  $\pm$  S.D.,  $n=3$ .

### 2.4.1.3. Discussion

Data for the compounds discussed here are listed in **Table 2-1**. A plot of IC<sub>50</sub> values against cell viability versus IC<sub>50</sub> values against *in vitro* phosphatase assay clearly showed that there is a correlation between inhibitory activity *in vitro* and in cells [**Figure 2-5 (A)**]. It has been reported that inhibition of high-level PPM1D expression arrests cell growth. These data indicated that the major target of these compounds is PPM1D. A shared framework and a carboxyl group contributed to the exertion of PPM1D specificity.

Substitution of two hydrophobic groups with hydrogen (SL-188) or a less bulky group (SL-189) substantially reduced inhibitory activity against PPM1D. These results indicated that hydrophobicity in this position is important for PPM1D inhibition *in vitro*. It has been reported that decreased molecular lipophilicity impairs affinity for the target protein (15). ClogD is the most commonly used measurement parameter for lipophilicity. Although a shared molecule showed slight inhibitory activity and it might be responsible for PPM1D specificity, SL-188 and SL-189 may have lipophilicity too low to fully interact with PPM1D in their current structure. A strong negative correlation exists between lipophilicity and anti-proliferative activity ( $R^2 = 0.94$ ) [**Figure 2-5 (B)**]. This result showed that compound lipophilicity is important for cell growth inhibition. However, there is a negative correlation ( $R^2 = 0.83$ ) when *in vitro* inhibition activity is plotted against ClogD [**Figure 2-5 (C)**], and it can be divided into a sterically bulky group and planar bulky group. The three-dimensionality and the presence of chiral centers correlate with success as drugs (16). These results suggested that sterically demanding hydrophobic groups, such as TES and TBS but not planar molecules, are suitable for

**Table 2-1.** Data list of SL compounds.



Compound	R <sup>1</sup>	R <sup>2</sup>	<i>in vitro</i> IC <sub>50</sub> (μM)	MCF7 cell IC <sub>50</sub> (μM)	ClogD	MW
SL-176	(C <sub>2</sub> H <sub>5</sub> ) <sub>3</sub> Si	<i>t</i> Bu(CH <sub>3</sub> ) <sub>2</sub> Si	0.27 ± 0.02	13.9 ± 0.15	3.89	456.8
SL-188	H	H	> 1	> 40	-2.08	228.3
SL-189	<i>t</i> Bu	<i>t</i> Bu	> 1	> 40	1.60	340.5
SL-194	(C <sub>2</sub> H <sub>5</sub> ) <sub>3</sub> Si	C <sub>6</sub> H <sub>5</sub> CH <sub>2</sub>	0.78 ± 0.03	27.9 ± 0.67	3.30	432.7
SL-195	(C <sub>2</sub> H <sub>5</sub> ) <sub>3</sub> Si	C <sub>6</sub> H <sub>5</sub> C(=O)	0.72 ± 0.20	25.6 ± 0.91	3.47	446.7
SL-196	<i>t</i> Bu(CH <sub>3</sub> ) <sub>2</sub> Si	<i>t</i> Bu(CH <sub>3</sub> ) <sub>2</sub> Si	0.20 ± 0.01	15.8 ± 1.08	3.70	456.8

Structure indicates the replaced moiety in this study.

ClogD value is measured using ChemAxon and chemicalize.com.



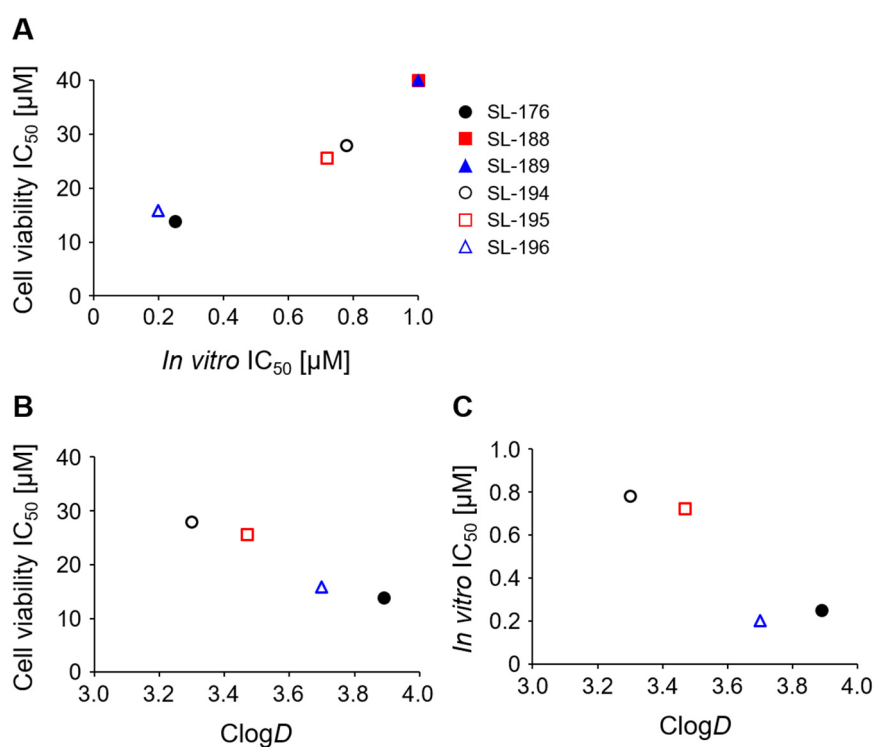


**Figure 2-5.** (A) A plot of IC<sub>50</sub> value of cell viability versus IC<sub>50</sub> value of *in vitro* phosphatase assay. SL-188 and SL-189 are plotted at highest tested concentration. (B) A plot of IC<sub>50</sub> value of cell viability assay versus ClogD.  $R^2 = 0.94$ . (C) A plot of IC<sub>50</sub> value of *in vitro* phosphatase assay versus ClogD.  $R^2 = 0.83$ . The black circle; SL-176, the red square; SL-188, the blue triangle; SL-189, the open black circle; SL-194, the open red square; SL-195 and the open blue triangle; SL-196.

interaction with the surface or hydrophobic pocket of the PPM1D protein. Studies of the stereoisomers of SL-176 may allow more appropriate inhibitors to be developed.

In summary, SAR studies revealed that two sterically demanding hydrophobic groups of SL-176 are necessary to inhibit PPM1D. A common structure is part of this functionality in that it exerts PPM1D specificity.

#### **2.4.2. Structure-activity relationship studies of hydrophilic group of SL-176**

##### **2.4.2.1. Effect of SL-175 and SL-177 on *in vitro* phosphatase activity and MCF7 cell viability**

To examine the effect of carboxylic acid on SL-176, I focused on the simple SARs of the carboxylic acid moiety of SL-176. SL-175 and SL-177 share a *trans*-decalin framework and two hydrophobic moieties (**Figure 2-6**). The reduction of the carboxylic acid to a primary alcohol (SL-175) or an amine (SL-177) was designed. The inhibitory activity of these compounds against PPM1D phosphatase was examined. I carried out *in vitro* PPM1D phosphatase assays and cell viability assays using the PPM1D-overexpressing MCF7 breast cancer cell line (**Figure 2-7 and 2-8**). SL-175 inhibited PPM1D at twice the IC<sub>50</sub> of SL-176 in *in vitro* phosphatase assay. Despite having a potent inhibitory effect on the phosphatase activity *in vitro*, SL-175 showed a lower inhibitory effect on MCF7 cell viability. SL-177 could strongly suppress MCF7 cell viability though SL-177 had little effect on inhibiting the phosphatase activity *in vitro*.

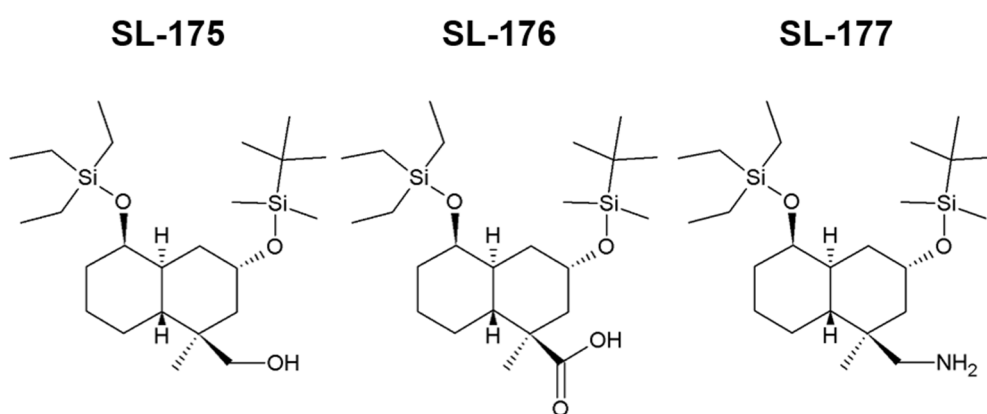


**Figure 2-6.** Structure of SL-175, SL-176 and SL-177

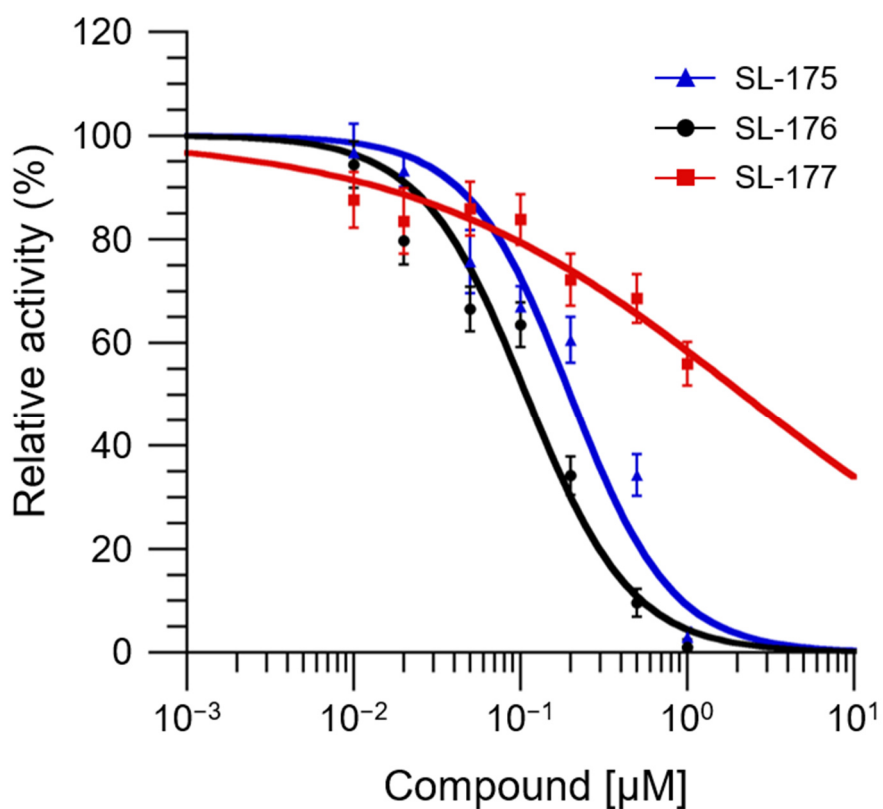


**Figure 2-7.** Inhibitory activity of SL-175, SL-176 and SL-177. *In vitro* phosphatase assay was carried out using His-PPM1D(1-420) enzyme and p53(10-21: pS15) peptide substrate. The blue triangle, the black circle and the red square indicate SL-175, SL-176 and SL-177, respectively. Data represent the mean  $\pm$  S.D.,  $n=9$ .

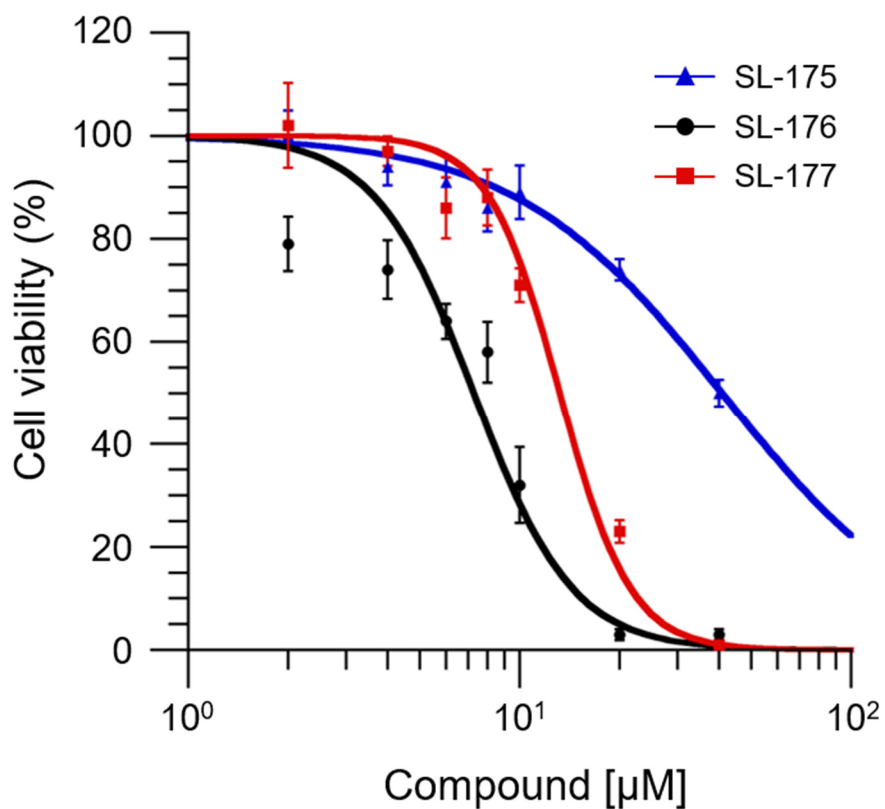


**Figure 2-8.** Cell viability of MCF7 cells under the treatment with a range of concentration of SL-175, SL-176 and SL-177. Cell viability was measured after treatment for 3 days. The blue triangle, the black circle and the red square indicate SL-175, SL-176 and SL-177, respectively. Data represent the mean  $\pm$  S.E.,  $n=9$ .

#### **2.4.2.2. Effect of SL-180 and SL-183 on *in vitro* phosphatase activity and MCF7 cell viability**

The simple SAR studies also raised the possibility that the amine would promote the cell viability inhibition of compounds that have the same structure as SL-176. These results prompted me to examine the effect of the amine form further. Based on the relationship between the different assays, I hypothesized that the amine allowed SL-177 to be better incorporated into the cell and accumulate to an effective concentration.

Next, I designed SL-180, the 2-aminoethyl-ester form of SL-176, and SL-183, the 4-aminobutyl-ester form of SL-176 (**Figure 2-9**). The carboxylic acid could cause metabolic instability and limit passive diffusion across biological membranes (17). Thus, the carboxylic acid was masked by an ester band. I also expected that an amine promoted the inhibition of cell viability. *In vitro* phosphatase assays showed that SL-180 and SL-183 had little effect on PPM1D (**Figure 2-10**). In contrast, SL-180 and SL-183 clearly showed a more potent inhibition with a steep slope than that of SL-176 (**Figure 2-11**).

#### **2.4.2.3. Effect of amine on intracellular uptake rate**

I focused on the examination of SL-183 due to its potent inhibitory activity in cells. To verify the hypothesis that the compound having an amine group is more easily incorporated into cells, I analyzed the intracellular uptake rate using fluorescein. MCF7 cells were treated with 5-carboxyfluorescein diacetate (5-CFDA) or 5-aminobutylfluorescein diacetate (5-ABFDA), and I observed fluorescence imaging at the indicated times (**Figure 2-12**). 5-ABFDA was incorporated into cells immediately after

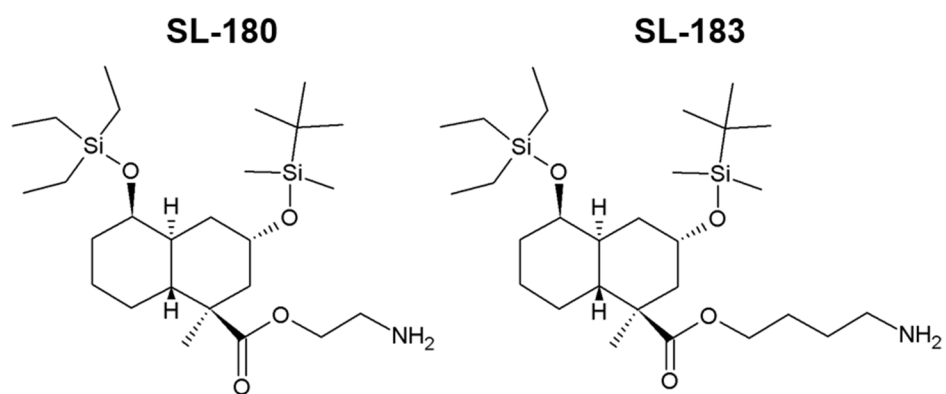


**Figure 2-9.** Structure of SL-180 and SL-183.

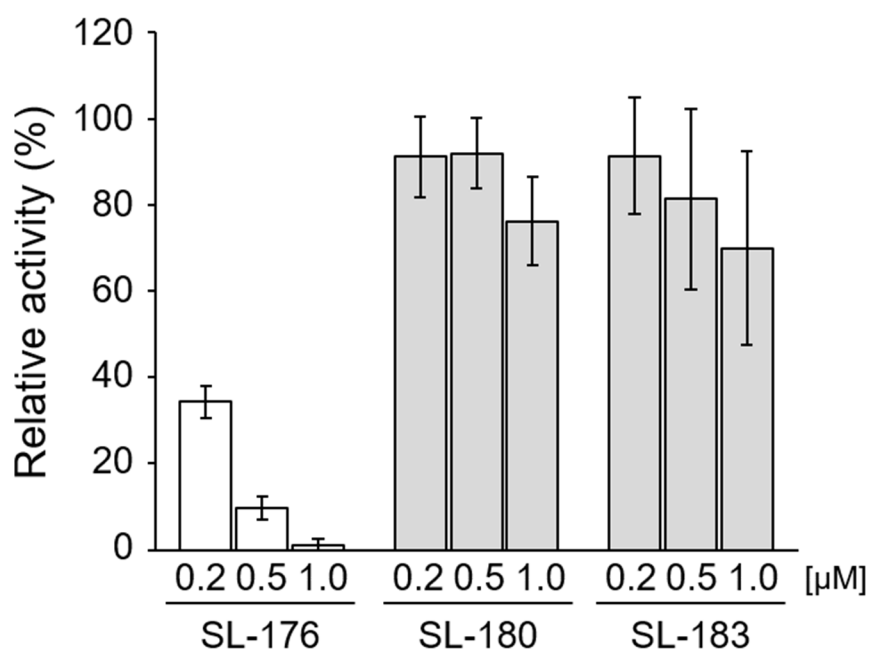


**Figure 2-10.** Inhibitory activity of SL-180 and SL-183. *In vitro* phosphatase assay was carried out using His-PPM1D(1-420) enzyme and p53(10-21: pS15) peptide substrate. Data represent the mean  $\pm$  S.D.,  $n=9$ .



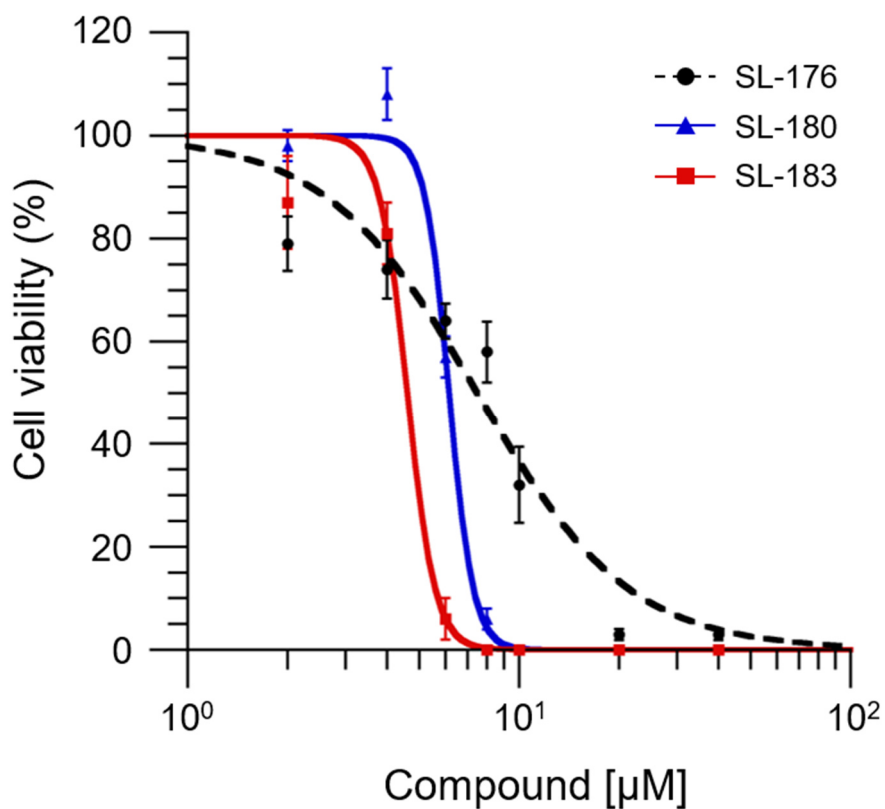
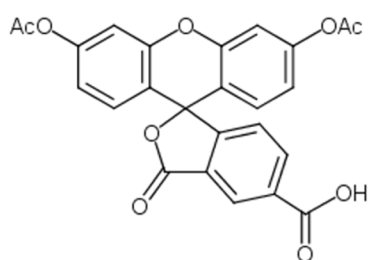


**Figure 2-11.** Cell viability of MCF7 cells under the treatment with a range of concentration of SL-180 and SL-183. Cell viability was measured after treatment for 3 days. The black circle, blue triangle and the red square indicate SL-176, SL-180 and SL-183, respectively. Data represent the mean  $\pm$  S.E.,  $n=6$  or 9.

**5-CFDA**



**5-ABFDA**

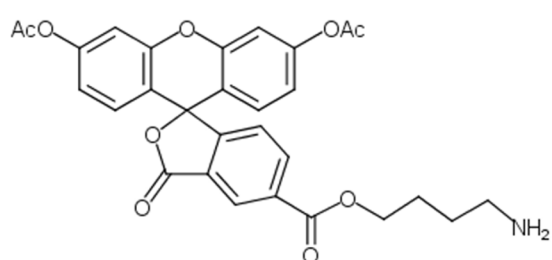


**Figure 2-12.** Structure of 5-CFDA and 5-ABFDA.

treatment and 5-ABFDA was incorporated approximately 100 times faster than 5-CFDA (**Figure 2-13**). This result showed that the difference between a carboxylic acid and an amine in the same intramolecular system affected the intracellular uptake of compounds. Thus, the 4-aminobutyl-ester moiety provided an advantage for incorporation into cells.

#### **2.4.2.4. Intracellular metabolite analysis of SL-183**

I conducted intracellular metabolite studies. MCF7 cells were treated with SL-183 for 6 h and the cell suspension was added to acetone. This crude cell extract was directly analyzed by LC-MS/MS. I observed the same MS fragment that corresponded to SL-176 with a molecular ion at  $m/z$  455.30 in MS and at  $m/z$  131.08 and 209.11 in MS/MS (**Figure 2-14 and 2-15**). These results showed that SL-183 was converted into SL-176 and functioned as a form of active SL-176 in the cells.

#### **2.4.2.5. PPM1D specificity of SL-183**

I analyzed the PPM1D specificity of SL-183 at the cellular level. I used H1299, which expresses normal levels of PPM1D, and a PPM1D-overexpressed cell line, namely H1299(PMD-9), which our laboratory established by transgenic HA-PPM1D (14). The anticancer agent etoposide suppressed H1299 cell viability significantly more than H1299(PMD-9) (**Figure 2-16**). SL-176 showed a much more potent inhibition of cell proliferation against H1299(PMD-9) cells than the H1299 cells (**Figure 2-16**). SL-183 inhibited H1299(PMD-9) cell viability significantly more than it inhibited H1299 cell viability. This result indicated that SL-183 exerted PPM1D specificity at a cellular level,

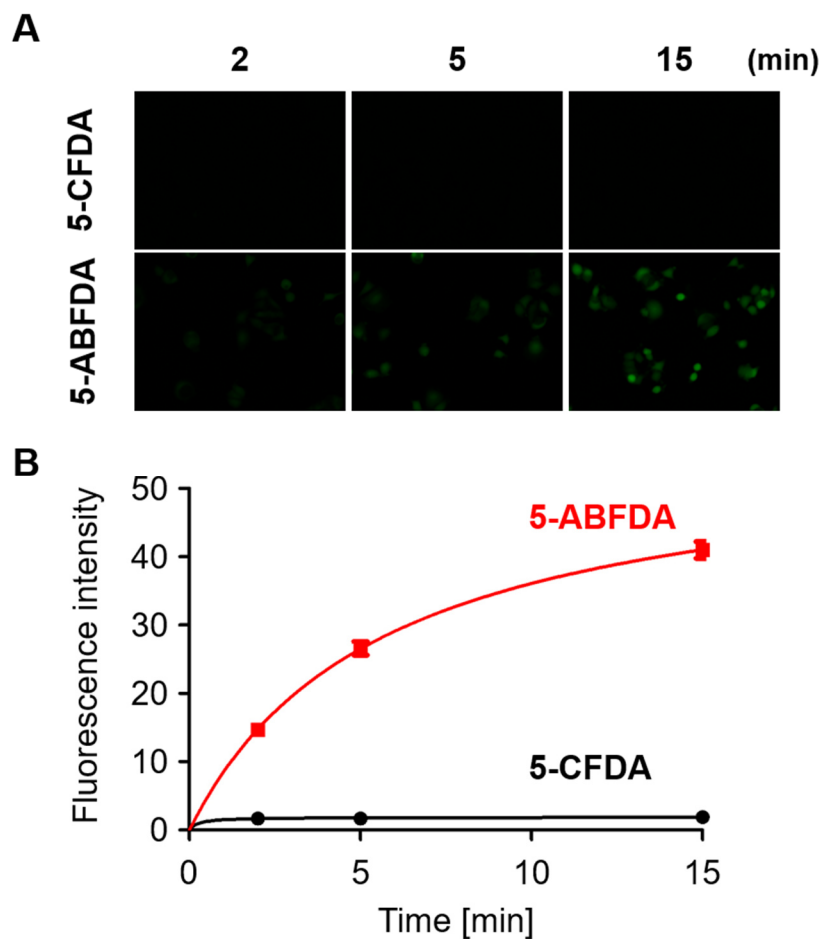


**Figure 2-13.** The time-dependent change of fluorescent compound in MCF7 cells. MCF7 cell was added with 0.1  $\mu$ M 5-CFDA or 5-ABFDA. Fluorescence images were obtained at indicated times by fluorescence microscopy (A). Kinetic modeling was fitted using GraphPad Prism 5 software (B).

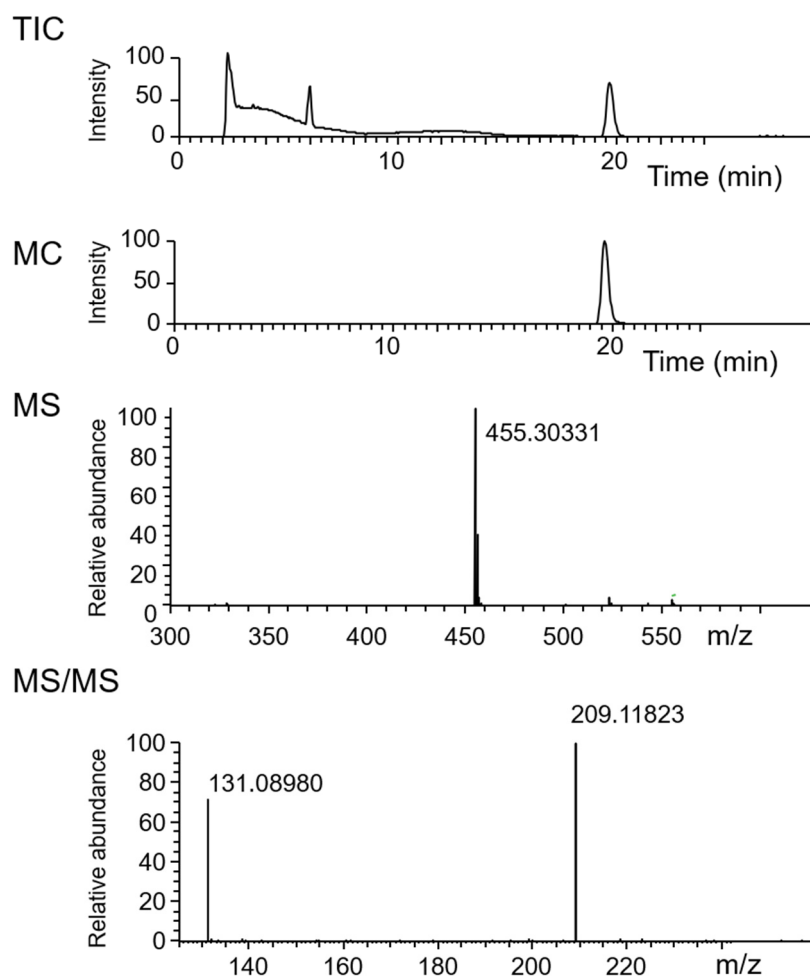


**Figure 2-14.** LC-MS/MS chromatograms of pure SL-176. The retention time is 19.66. MS spectra show a mass of  $m/z$  455. In the MS/MS spectra, two ions were detected:  $m/z$  131 and 209. TIC, Total ion current chromatogram; MC, mass chromatogram.

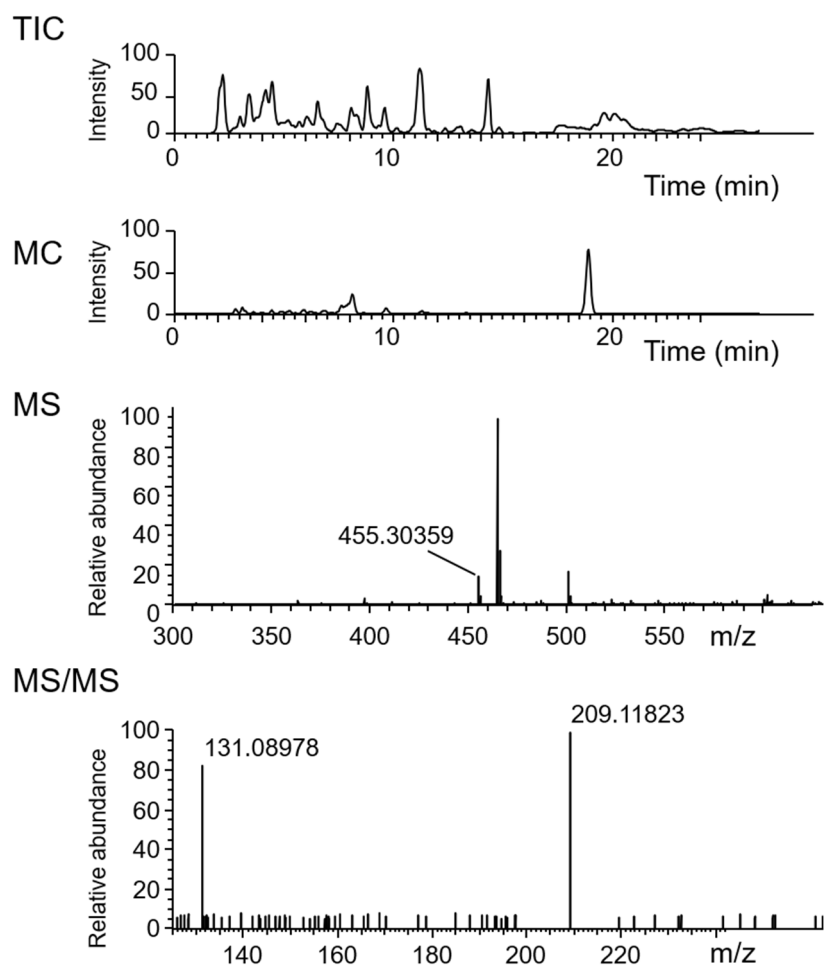


**Figure 2-15.** LC-MS/MS chromatograms of SL-183 treated MCF7 cell. The retention time is 18.92. MS spectra show a mass of  $m/z$  455. In the MS/MS spectra, two ions were detected:  $m/z$  131 and 209. TIC, Total ion current chromatogram; MC, mass chromatogram.

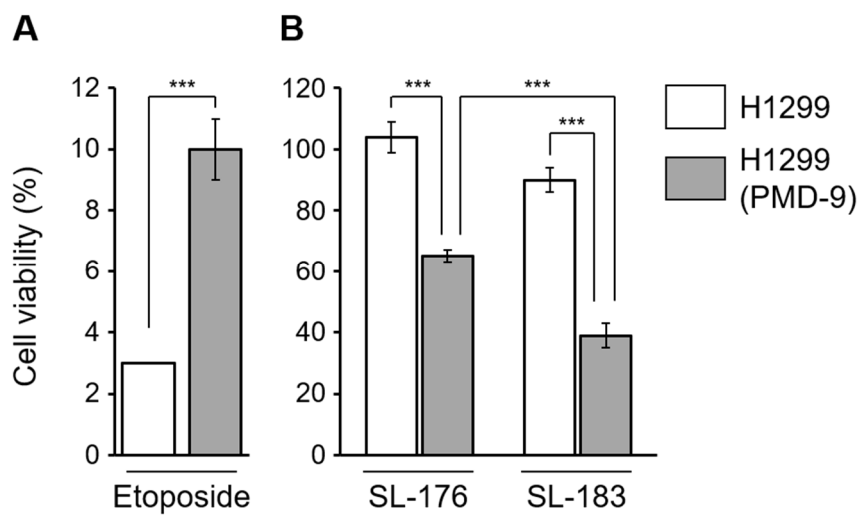


**Figure 2-16.** Cell viability of H1299 and H1299(PMD-9) cells. Cell viability was measured after treatment for 3 days. The concentration of etoposide is 10 mg/ ml (A) and SL-176 and SL-183 is 10  $\mu$ M (B), respectively. Data represent the mean  $\pm$  S.D.,  $n=3$ . \*\*\* $< 0.001$ ,  $t$ -test.

whereas its inhibitory activity was moderate.

### 2.4.3. Discussion

In this study, SAR showed that the replacement of the carboxylic acid into the amino alkyl-ester promoted inhibitory activity against MCF7 cell viability. The carboxylic acid group is an important pharmacophore due to establishment of relatively strong electrostatic interactions and hydrogen bonds (17). However, the presence of carboxylic acid can decrease the passive diffusion across membranes and increase drug toxicities due to the metabolism of the carboxylic acid moiety. Thus, the replacement of the carboxylic acid group and masking of this moiety as an ester are effective strategies. Moreover, one of the key parameters for defining lipophilicity is  $\log D$ . It is well known that high-permeability compounds had  $\log D$  values of between 0 and 3, and low-permeability compounds had  $\log D$  values  $< -1.5$  or  $> 4.5$  (13). The  $\text{Clog}D$  of these compounds is a relatively good value (Table 2-2).

Treatment with SL-183 for identical cell lines expressing different PPM1D protein levels significantly decreased cell viability, depending on the PPM1D expression level. Etoposide, a commonly used anticancer agent, is less effective in H1299(PMD-9) cells, suggesting that the PPM1D-overexpressed cancer has a high malignancy. In contrast, SL-176 and SL-183 effectively decreased cell viability. This result indicated that these inhibitors are attractive molecule-targeting drugs against cancer cells in which PPM1D is overexpressed.

Treatment with etoposide also showed that the drug sensitivity of H1299(PMD-



9) did not increase due to transformation. This result supported that SL-183 decreased the cell viability via a specific inhibition of PPM1D at the cellular level.

From the sigmoidal proliferation inhibition curve in Figure 2-11, one can see that the Hill coefficient  $\gg 1$ , indicating that SL-180 and SL-183 act via a positive cooperative mechanism. This positive effect can be explained by an increase in potential interaction sites between PPM1D and these compounds, and the alteration of intracellular concentrations of the compound. The C-terminal domain of PPM1D was not expressed in *in vitro* phosphatase assay. Because the Hill coefficient reflects interaction, there is a possibility that these compounds also interact with the C-terminal domain (18). Although general passive transport depends entirely on local concentration gradients, the driving force of membrane transport cannot be simplified as a concentration gradient when solubility is altered by decreased permeability (19). Metabolite analysis revealed that SL-183 was converted to SL-176 in the cells. Given that the 4-aminobutylester promoted the intracellular uptake rate, an unequilibrated concentration change of the active compound in cells might confer positive cooperation for PPM1D inhibition.

An overall model for the mechanism of intracellular activation of SL-183 is shown in **Figure 2-17**. SL-183, having 4-aminobutylester, was immediately incorporated into cells and converted into SL-176. SL-176 accumulated due to the lower cell membrane permeability of its carboxylic acid. SL-176 effectively decreased cell viability, depending on PPM1D expression level.

Our group has previously demonstrated that two hydrophobic moieties are responsible for the inhibitory activity of SPI-001 (10). In this study, I showed that the

**Table 2-2.** Data list of SL compounds. Structure indicates the replaced moiety in this study.

<b>Compound</b>	<b>Structure</b>	<b><i>in vitro</i> IC<sub>50</sub> (nM)</b>	<b>MCF7 cell IC<sub>50</sub> (μM)</b>	<b>ClogD</b>	<b>MW</b>
SL-175	CH <sub>2</sub> OH	216 ±37	41.3 ±3.6	6.07	442.6
SL-176	COOH	110 ±15	7.4 ±0.8	3.89	456.8
SL-177	CH <sub>2</sub> NH <sub>2</sub>	>1000	13.5 ±0.6	3.56	441.8
SL-180	C(=O)O-(C <sub>2</sub> H <sub>2</sub> )NH <sub>2</sub>	>1000	6.2 ±0.1	4.02	499.9
SL-183	C(=O)O-(C <sub>4</sub> H <sub>8</sub> )NH <sub>2</sub>	>1000	4.6 ±0.2	3.63	527.9

ClogD value is measured using ChemAxon and chemicalize.com.

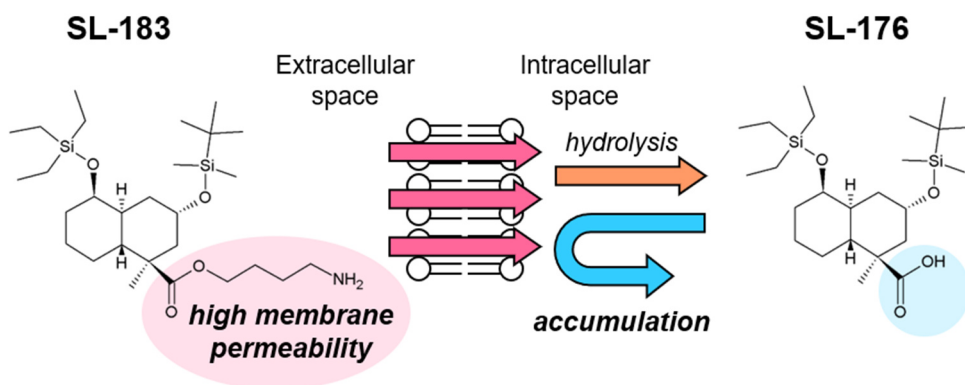


**Figure 2-17.** Mechanism model of intracellular activation of SL-183. SL-183 effectively incorporated into cells and converted into SL-176. SL-176 was accumulated and decreased cell viability.

opposite side moiety also affects inhibitory activity. The molecular weight >500 is poor for passive passage. Further studies are needed to decrease the lipophilicity while maintaining the inhibitory character by advanced SAR studies of these moieties. In conclusion, the introduction of an amino alkyl-ester into SL-176 improved its inhibitory activity and provided an effective strategy for development of new inhibitors for PPM1D.

## 2.5. Reference

1. Lu, X., Nannenga, B., and Donehower, L. A. (2005) PPM1D dephosphorylates Chk1 and p53 and abrogates cell cycle checkpoints. *Genes Dev.* **19**, 1162–1174
2. Takekawa, M., Adachi, M., Nakahata, A., Nakayama, I., Itoh, F., Tsukuda, H., and Imai, K. (2000) p53-inducible Wip1 phosphatase mediates a negative feedback regulation of p38 MAPK-p53 signaling in response to UV radiation. *EMBO J.* **19**, 6517–6526
3. Shreeram, S., Demidov, O. N., Hee, W. K., Yamaguchi, H., Onishi, N., Kek, C., Timofeev, O. N., Dudgeon, C., Fornace, A. J., Anderson, C. W., Minami, Y., Appella, E., and Bulavin, D. V. (2006) Wip1 Phosphatase Modulates ATM-Dependent Signaling Pathways. *Mol. Cell.* **23**, 757–764
4. Li, J., Yang, Y., Peng, Y., Austin, R. J., Van Eyndhoven, W. G., Nguyen, K. C. Q., Gabriele, T., McCurrach, M. E., Marks, J. R., Hoey, T., Lowe, S. W., and Powers, S. (2002) Oncogenic properties of PPM1D located within a breast cancer amplification epicenter at 17q23. *Nat. Genet.* **31**, 133–134
5. Rauta, J., Alarmo, E. L., Kauraniemi, P., Karhu, R., Kuukasjärvi, T., and Kallioniemi, A. (2006) The serine-threonine protein phosphatase PPM1D is frequently activated through amplification in aggressive primary breast tumours. *Breast Cancer Res. Treat.* **95**, 257–263
6. Yu, E., Ahn, Y. S., Jang, S. J., Kim, M. J., Yoon, H. S., Gong, G., and Choi, J. (2007) Overexpression of the wip1 gene abrogates the p38 MAPK/p53/Wip1

- pathway and silences p16 expression in human breast cancers. *Breast Cancer Res. Treat.* **101**, 269–278
7. Cerami, E., Gao, J., Dogrusoz, U., Gross, B. E., Sumer, S. O., Aksoy, B. A., Jacobsen, A., Byrne, C. J., Heuer, M. L., Larsson, E., Antipin, Y., Reva, B., Goldberg, A. P., Sander, C., and Schultz, N. (2012) The cBio Cancer Genomics Portal: An open platform for exploring multidimensional cancer genomics data. *Cancer Discov.* **2**, 401–404
  8. Hirasawa, A., Saito-Ohara, F., Inoue, J., Aoki, D., Susumu, N., Yokoyama, T., Nozawa, S., Inazawa, J., and Imoto, I. (2003) Association of 17q21-q24 gain in ovarian clear cell adenocarcinomas with poor prognosis and identification of PPM1D and APPBP2 as likely amplification targets. *Clin. Cancer Res.* **9**, 1995–2004
  9. Saito-Ohara, F., Imoto, I., Inoue, J., Hosoi, H., Nakagawara, A., Sugimoto, T., and Inazawa, J. (2003) PPM1D is a potential target for 17q gain in neuroblastoma. *Cancer Res.* **63**, 1876–1883
  10. Yagi, H., Chuman, Y., Kozakai, Y., Imagawa, T., Takahashi, Y., Yoshimura, F., Tanino, K., and Sakaguchi, K. (2012) A small molecule inhibitor of p53-inducible protein phosphatase PPM1D. *Bioorganic Med. Chem. Lett.* **22**, 729–732
  11. Lipinski, C. A., Lombardo, F., Dominy, B. W., and Feeney, P. J. (2012) Experimental and computational approaches to estimate solubility and

- permeability in drug discovery and development settings. *Adv. Drug Deliv. Rev.* **64**, 4–17
12. Lipinski, C. A. (2004) Lead- and drug-like compounds: The rule-of-five revolution. *Drug Discov. Today Technol.* **1**, 337–341
  13. Krämer, S. D. (1999) Absorption prediction from physicochemical parameters. *Pharm. Sci. Technol. Today.* **2**, 373–380
  14. Ogasawara, S., Kiyota, Y., Chuman, Y., Kowata, A., Yoshimura, F., Tanino, K., Kamada, R., and Sakaguchi, K. (2015) Novel inhibitors targeting PPM1D phosphatase potently suppress cancer cell proliferation. *Bioorganic Med. Chem.* **23**, 6246–6249
  15. Chène, P. (2006) Drugs targeting protein-protein interactions. *ChemMedChem.* **1**, 400–411
  16. Lovering, F., Bikker, J., and Humblet, C. (2009) Escape from flatland: Increasing saturation as an approach to improving clinical success. *J. Med. Chem.* **52**, 6752–6756
  17. Carlo, B., Donna, M. H., and Amos, B. Smith, L. (2013) Carboxylic Acid (Bio)isosteres in Drug Design. *ChemMedChem.* **8**, 385–395
  18. Weiss, J. N. (1997) The Hill equation revisited: uses and misuses. *Faseb J.* **11**, 835–841
  19. Borbás, E., Sinkó, B., Tsinman, O., Tsinman, K., Kiserdei, É., Démuth, B., Balogh, A., Bodák, B., Domokos, A., Dargó, G., Balogh, G. T., and Nagy, Z. K. (2016) Investigation and mathematical description of the real driving force of

passive transport of drug molecules from supersaturated solutions. *Mol. Pharm.*

**13**, 3816–3826



### 3. Role of PPM1D in differentiation induction on NT2/D1 cells

#### 3.1. Abstract

The Ser/Thr protein PPM1D (Wip1 and PP2C $\delta$ ) is induced by p53 in response to stress. Activation of PPM1D through various mechanisms promotes the tumorigenic potential of various cancers by suppressing p53 and other DNA damage response proteins. Recent studies have revealed the functions of PPM1D in various cellular physiology and pathological conditions other than DNA damage response. Although PPM1D is receiving increasingly great attention, the involvement of PPM1D in any process, such as differentiation induction, is still unclear.

In this study, I examined the role of PPM1D in the RA signaling pathway using the human embryonic carcinoma cell line NT2/D1. The RA signaling pathway is involved in processes such as cell development and differentiation. PPM1D knockdown decreased alkaline phosphatase activity in NT2/D1 cells, suggesting that cell differentiation was induced. PPM1D knockdown decreased levels of the stem cell marker Oct-4 protein. These results suggested that PPM1D is an important factor that maintains an undifferentiated state in NT2/D1 cells. The treatment of the RA decreased *POU5F1* (Oct-4) after 3 days, whereas *PPM1D* mRNA levels gradually increased immediately after treatment. Treatment with the PPM1D inhibitor SL-176 decreased Oct-4 protein levels. Moreover, SL-176 promoted the decrease in expression of the *POU5F1* gene by RA treatment. The PPM1D mutant was expressed as enhanced RA-induced cell differentiation. Overall, these results indicated that PPM1D activity was involved in

maintaining an undifferentiated state in NT2/D1 cells, and PPM1D can upon the RA pathway.

### 3.2. Introduction

The protein phosphatase PPM1D negatively regulates the genotoxic stress response by dephosphorylation of various proteins. Previous studies have mainly highlighted the role of PPM1D in tumorigenesis (1, 2). It has been reported that PPM1D is involved in the regulation of STATs, mTOR, Sonic Hedgehog, Notch, and Wnt signal pathways other than the DNA damage response (3). Additionally, *Ppm1d* knockout mice showed cell cycle abnormality and failure of male reproductive organs and the immune response (4). Recently, several studies have also reported the functions of PPM1D under in a wide range of physiological conditions, such as cell senescence, neurogenesis, obesity, atherosclerosis, liver regeneration, and maintenance of stemness (5–8). Particularly in stem cells, PPM1D expression suppresses senescence-like growth arrest in human mesenchymal stem cells and maintains their differentiation potential due to inactivation of the stress signaling pathway (9). Moreover, overexpression of PPM1D increased neural stem/progenitor cell numbers in aged mice and maintained neuronal differentiation (10). This evidence has implicated PPM1D in maintaining cellular homeostasis through cell cycle control. Conceptually, cancer ensues upon dysregulated activation of signaling cascades, such as the MAPKs, PI3K/Akt, and Wnt signal pathways. Based on the critical role of PPM1D substrates in tumorigenesis, it is rational that PPM1D at the physiological protein level is involved in cell differentiation, whereas the dysregulation of PPM1D facilitates carcinogenesis.

Cell differentiation is highly regulated by intrinsic and extrinsic signaling pathways and the subsequent activation of transcription. With the study of cell biology,

many signaling cascades that control cell differentiation are being uncovered.

In this study, I examined the role of PPM1D in the RA signaling pathway, which is one of the most important pathways for development and cell differentiation. I used the human embryonic carcinoma cell line NT2/D1, which are available for the study of cellular differentiation.

### **3.3. Experimental procedures**

#### **3.3.1. Cell lines and materials**

NT2/D1 (NTERA-2 cl. D1) human teratocarcinoma cells were obtained from American type tissue culture collection (ATCC) (Rockville, MD, USA). Rabbit polyclonal anti-PPM1D was prepared as previously described (11). Other antibodies used include: anti-Oct-4 (C-10) (sc-5279) and anti-GAPDH (FL-335) (sc-25778) from Santa Cruz Biotechnology; anti-rabbit IgG HRP-linked Antibody (7074) from Cell Signaling Technology; and anti-mouse IgG HRP-linked Antibody (NA931) from GE healthcare. Secondary antibodies for immunocytochemistry included Alexa Fluor488 goat anti-mouse IgG and Alexa Fluor568 goat anti-rabbit IgG from Invitrogen. PPM1D inhibitor SL-176 was obtained from Laboratory of Organic Chemistry II (Faculty of Science, Hokkaido University).

#### **3.3.2. Cell manipulation**

NT2/D1 cells were cultured in Dulbecco's modified Eagles medium supplemented with 10% v/v fetal bovine serum with 100 µg/ml of streptomycin and 100 units/ml of penicillin at 37 °C in a humidified 5% CO<sub>2</sub> incubator. NT2/D1 cells were plated onto 35 mm dish with 1.5 ml of medium and incubated for 24 h before operation. Transient transfection of siRNA for PPM1D was carried out using Lipofectamine RNAiMAX Regent (Invitrogen) following the manufacturer's instructions. PPM1D siRNAs are 5'-GAAGUGGACAAUCAGGGAAACUUUACCA-3' and 5'-

UAAAGUUUCCCUGAUUGUCCACUUC-3'. Cells were treated with RA and inhibitor after 24 h of transfection. Change and refresh medium containing RA every 2 days. Plasmid transfection was conducted using Lipofectamine 2000 (Invitrogen). The plasmids were used for transient expression of PPM1D: phCMV-mCherry-NLS-2A-PPM1D(1-605) and phCMV-mCherry-NLS-2A-PPM1D(1-605)(D314A).

### **3.3.3. Alkaline phosphatase staining**

NT2/D1 cells were plated onto 10 cm dish and transfected with siRNA for PPM1D after 24 h. After 24 h, the cells were reseeded onto 24 well plate. After 36 h, the cell RA group was treated with 10  $\mu$ M RA for 3 days. Alkaline phosphatase activity was determined using Alkaline Phosphatase Staining Kit II (Stemgent) following the manufacturer's instructions.

### **3.3.4. Western blotting**

All cells were rinsed with PBS twice and lysed in 1x sample buffer (50 mM Tris-HCl, pH 6.8, 10% Glycerol, 2% SDS). Cell lysates were normalized for total protein using BCA Protein Assay Kit (Pierce) and then added 2-mercaptoethanol to 6%. Protein were separated by SDS-PAGE and transferred to polyvinylidene difluoride membranes. Proteins were detected by enhanced chemiluminescence with the above antibodies.

### 3.3.5. Immunofluorescence

NT2/D1 cells were plated on glass coverslips on 35 mm dish for 24 h. Cells were fixed with 3.5% formaldehyde for 15 min, washed in PBS, permeabilized with 0.2% Triton X-100/PBS for 5 min, and blocked with 10% FBS/PBS for 1 h. After incubation with primary antibodies overnight at 4 °C, cells were stained with secondary antibodies and 4',6-diamidino-2-phenylindole. Cells were observed by fluorescence microscopy (BZ-9000, KEYENCE).

### 3.3.6. Quantitative RT-PCR

All cells were rinsed with PBS twice and harvested in TRIzol (Life technologies) after treatment with the compounds. Total RNA was transcribed using the PrimerScript II 1st strand cDNA Synthesis Kit (TaKaRa) with random hexamer primers following the manufacturer's instructions. qRT-PCR was performed using a CFX96 Touch real-time PCR detection system (Bio-Rad) using iTaq Universal SYBR Green Supermix (Bio-Rad). Primers used include. Primer for PPIA is 5'CAAATGCTGGACCCAACACA3' and 5'TGCCATCCAACCACTCAGTC3'; for POU5F1 is 5'AGCAAAACCCGGAGGAGT3' and 5'CCACATCGGCCTGTGTATATC3'; for PPM1D is 5'ACCAGTCAAGTCACTGGAGG3' and 5'ATTGCTACGAACCAGGGCAG3'. Transcript levels were normalized to peptidylprolyl isomerase (PPIA) mRNA expression. Fold changes were calculated by the Ct method.

### **3.4. Results**

#### **3.4.1. Effect of PPM1D knockdown on alkaline phosphatase activity in NT2/D1 cells**

The NT2/D1 cells have been shown to differentiate along the neuronal lineage by treatment with RA (12). I carried out alkaline phosphatase (AP) staining, a marker of the undifferentiated state. Most of the control cells were positive for AP, whereas cells treated with RA for 3 days showed negative AP activity (**Figure 3-1**). To examine the role of PPM1D in NT2/D1 cells, I performed PPM1D knockdown using siRNA. PPM1D knockdown also decreased in AP activity.

#### **3.4.2. Effect of PPM1D knockdown on Oct-4 expression levels in NT2/D1 cells**

Stemness factors, such as Oct-4 and NONOG, are expressed in NT2/D1 cells (13). I confirmed the effect of treatment with RA and PPM1D knockdown on Oct-4 expression levels by western blot analysis. Treatment with RA decreased the expression level of Oct-4 (**Figure 3-2**). I confirmed that PPM1D knockdown also induced a decrease of Oct-4 protein. These results showed that PPM1D knockdown induced differentiation in NT2/D1 cells. This result suggested that PPM1D maintain the undifferentiated state on NT2/D1 cells.

#### **3.4.3. RA-induced changes in gene and protein expression**

To characterize the function of PPM1D in the RA signaling pathway, I analyzed *PPM1D* mRNA and protein level. The administration of RA decreased *POU5F1* (which



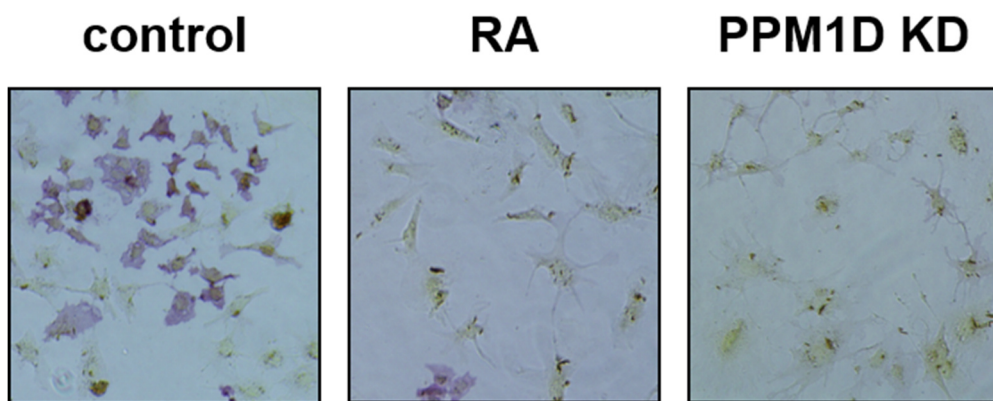


**Figure 3-1.** Effect of PPM1D knockdown on alkaline phosphatase activity in NT2/D1 cell. NT2/D1 cells were transfected with PPM1D siRNA (PPM1D KD panel) or vehicle (control and RA panels). The cells were reseeded after 24h. After 36 h, the RA cell group was treated with 10  $\mu$ M RA for 3 days. Representative images of the stained cells are shown at x10 magnification.

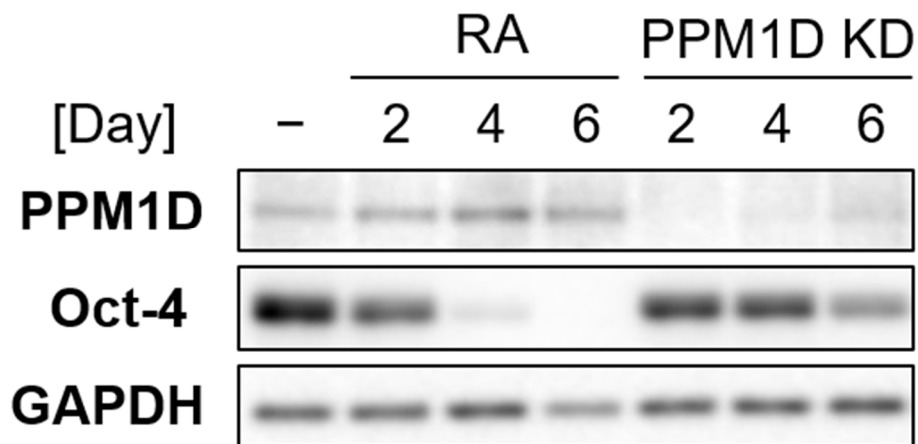


**Figure 3-2.** Effect of PPM1D knockdown on Oct-4 expression levels. NT2/D1 cells were transfected with PPM1D siRNA (KD lanes) or vehicle (RA lanes). the RA cell group was treated with 10  $\mu$ M RA for the indicated days. The cells were immunoblotted for PPM1D, Oct-4 and GAPDH (used as a loading control). Data are representative of at least three independent experiments.

encodes Oct-4) after 3 days of treatment, whereas *PAX6* which is a neural marker dramatically increased after 4 days of treatment (**Figure 3-3**). *PPM1D* mRNA levels gradually increased after treatment with RA. Consistent with the mRNA results, Oct-4 protein levels dramatically decreased after 4 days of treatment (**Figure 3-4**). *PPM1D* protein levels initially increased and then decreased. I also carried out immunofluorescence staining to confirm the expression level and localization. Both Oct-4 and *PPM1D* signals were observed in the nucleus of untreated cells, and most of cells treated with RA lost Oct-4 expression (**Figure 3-5**). The *PPM1D* localization was not changed by RA treatment.

#### **3.4.4. Effect of SL-176 treatment on RA-induced differentiation induction**

Next, I analyzed the function of *PPM1D* on RA-induced differentiation induction by a biochemical approach. The *PPM1D* inhibitor SL-176 inhibited *PPM1D* phosphatase activity *in vitro*. SL-176 suppressed *PPM1D*-overexpressed cell viability rather than normal level expressed cell viability (14). Treatment with SL-176 slightly decreased Oct-4 protein levels (**Figure 3-6**). Combined treatment with RA and SL-176 decreased *POU5F1* levels after 12 hours compared with RA treatment (**Figure 3-7**). This effect was observed up to 2 days after exposure. No differences were observed between RA treatment and combined treatment at 4 and 6 days. These results suggested that the effect of SL-176 on the regulation of Oct-4 mRNA was exerted in the early step of the RA signaling.

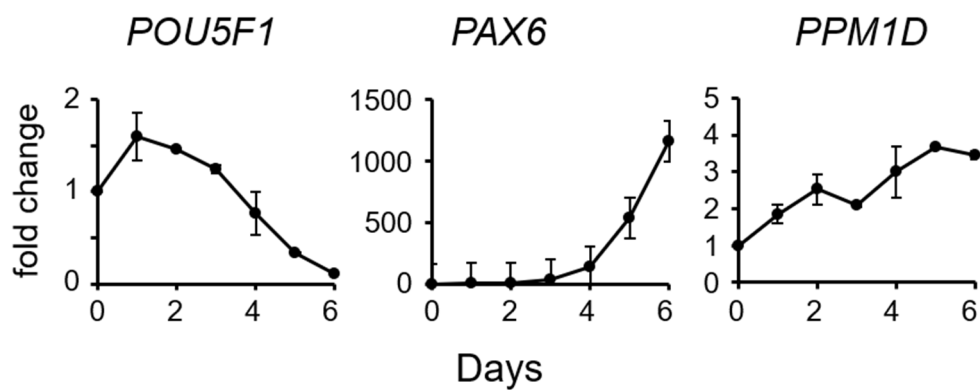


**Figure 3-3.** RA-induced cell differentiation. NT2/D1 cells were treated with 10  $\mu$ M RA for the indicated days after exposure. Quantitative RT-PCR for the indicated genes and normalized with PPIA. Fold-change was determined compare with day 0. Values are the mean  $\pm$  range of duplicates. Data are representative of at least three independent experiments.

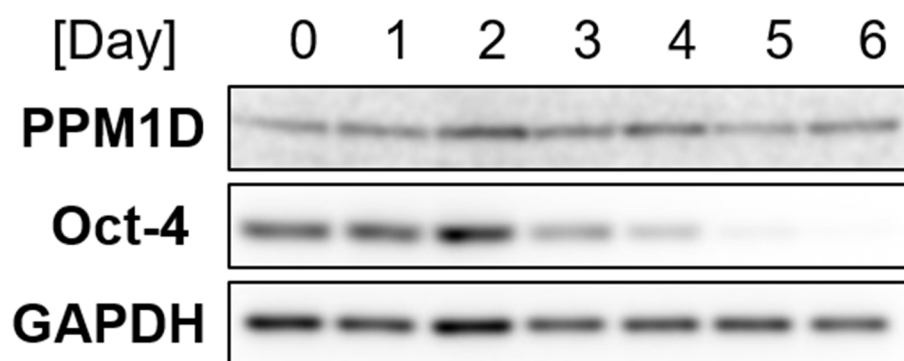


**Figure 3-4.** RA-induced cell differentiation. NT2/D1 cells were treated with 10  $\mu$ M RA for the indicated days after exposure. Immunoblot of the indicated proteins. GAPDH was used as loading control. Data are representative of at least three independent experiments.

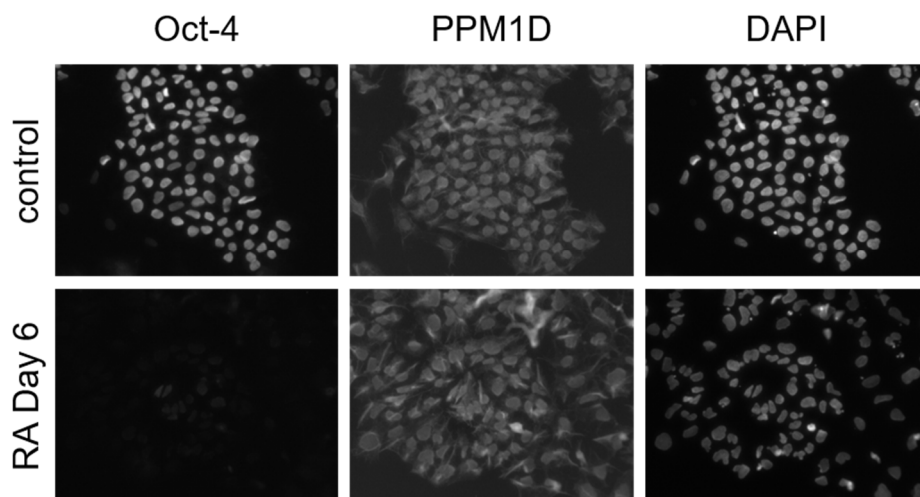


**Figure 3-5.** RA-induced cell differentiation. NT2/D1 cells were treated with 10  $\mu$ M RA for the indicated days after exposure. The cells were fixed and stained with the indicated proteins. Images at x40 magnification are representative of at least two experiments.

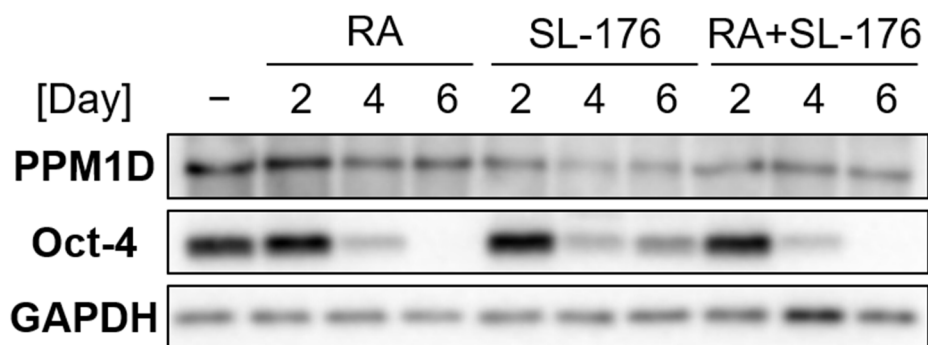


**Figure 3-6.** Effect of SL-176 treatment on Oct-4 expression level. NT2/D1 cells were treated with 10  $\mu$ M RA or/and 7.5  $\mu$ M RA SL-176 for the indicated days after treatment. Data are representative of at least three independent experiments.

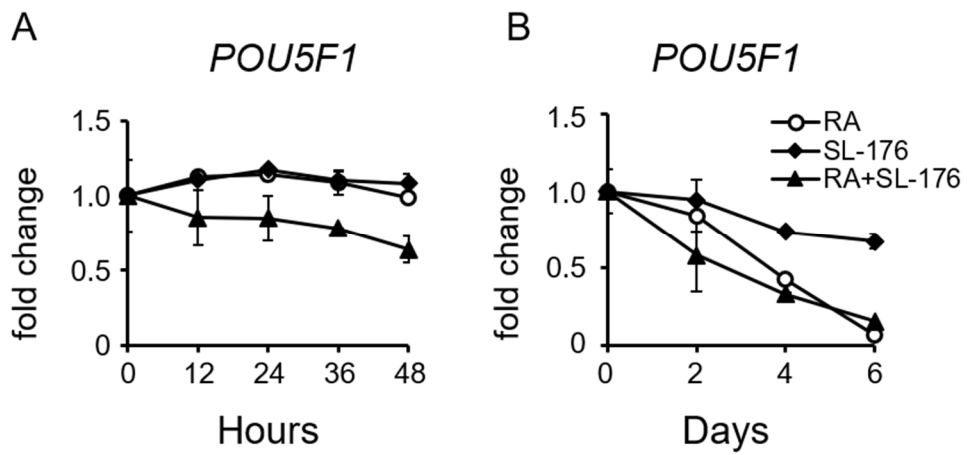


**Figure 3-7.** Effect of SL-176 treatment on RA-induced cell differentiation. NT2/D1 cells were treated with 10  $\mu$ M RA or/and 7.5  $\mu$ M RA SL-176 for the indicated days after treatment. Values are the mean  $\pm$  range of duplicates. Data are representative of at least three independent experiments.



### 3.4.5. Effect of PPM1D overexpression on RA-induced differentiation induction

To analyze the effect of PPM1D overexpression on RA-induced differentiation, I examined the Oct-4 expression level by immunocytochemistry. I constructed vectors that contain mCherry-NLS and a wild-type PPM1D605 (PPM1D(WT)) linked by a 2A self-processing peptide sequence. The expression level of Oct-4 in mCherry-expressed cells was quantified by fluorescent immunostaining after transfection. The D314 residue in the active site of PPM1D is structurally linked to its metal ion-binding site, PPM1D(D314A) (PPM1D(DA)) is an inactive mutant. In the absence of RA, Oct-4 expression levels in PPM1D(DA)-expressing cells significantly decreased with respect to levels in the WT-expressed cells and controls (**Figure 3-8**). In the presence of RA, Oct-4 levels drastically decreased in the WT-expressed cells and controls. The mutant further reduced the Oct-4 expression in RA-treated cells. These results again suggested that PPM1D activity is required to maintain an undifferentiated state and that decreased PPM1D activity enhanced RA-mediated induction of cell differentiation.

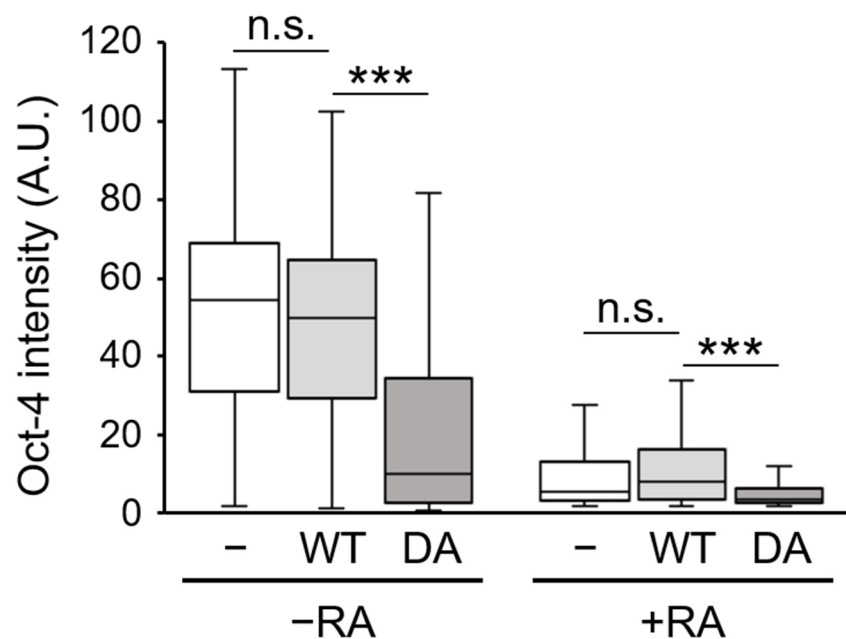


**Figure 3-8.** Effect of PPM1D overexpression on RA-induced cell differentiation. NT2/D1 cells were transfected with a plasmid carrying mCherry-NLS, mCherry-NLS-2A-PPM1D605(WT) and mCherry-NLS-2A-PPM1D605(D314A) (PPM1D(DA)). After 24 h, the cells were treated with 10  $\mu$ M RA. After 3 days, the cells were fixed and stained with anti-Oct-4 antibody. A box plot of the fluorescence intensity of Oct-4 in mCherry expressing cells regarded as expression of PPM1D protein was measured by fluorescent microscopy. Numbers of analyzed cells; -RA, mCherry-NLS (n=167); PPM1D(WT) (n=272); PPM1D(DA) (n=119); +RA, mCherry-NLS (n=200); PPM1D(WT) (n=270); PPM1D(DA) (n=205). \*\*\* $P < 0.001$ , n.s.  $P > 0.01$ , Mann-Whitney's U test.

### 3.5. Discussion

In this study, I demonstrated that PPM1D knockdown induced differentiation in NT2/D1 cells. This result suggested that PPM1D plays an important role in maintaining the undifferentiated state. Several reports indicated the relationship between the functions of PPM1D in stem cells and cell senescence. PPM1D knockout mouse embryonic fibroblasts showed premature senescence via activation of p53 under physiological oxygen levels (15). In a study using human mesenchymal stem cells, premature senescence obstructed the maintenance of constant cell growth and the ability to differentiate. Expression of PPM1D suppressed p16INK4a expression, which is one cause of premature cell growth arrest, via p38 MAPK inactivation in mesenchymal stem cells (9). Overexpression of PPM1D rescued the functional neural stem/progenitor cell differentiation in the aged-mice subventricular zone via Wnt signaling (10). Conversely, PPM1D knockout hematopoietic stem cells impaired the regenerative capacity and showed aging-like phenotypes, whereas the markers for cell senescence did not detect any difference compared with the wild type (16). This impaired functionality was not due to cell senescence but rather reduced differentiation capacity. It is interesting to examine the markers of cellular senescence in NT2/D1 cell differentiation, but further studies are needed to identify the molecular mechanism of stemness maintenance by PPM1D.

The treatment of SL-176 affected Oct-4 mRNA levels in RA-mediated differentiation. This result suggested that PPM1D is involved in regulation of Oct-4 transcriptional levels. Precise levels Oct-4 expression is one of the essential factors for maintaining the pluripotency of embryonic stem cells. Several studies showed that

phosphorylation of Oct-4 controlled the function of Oct-4 (17, 18). The serine 229 phosphorylation of Oct-4 sterically interferes with both its ability to bind DNA and form a homodimer assembly (19). These results suggested that the phosphorylation level of Oct-4 can influence its transcription. In this study, I showed that expression of PPM1D induced a slight decrease in Oct-4 expression compared with the controls. Moreover, expression of PPM1D(DA) dramatically decreased Oct-4 expression. The D314 residue is expected to occupy the active site, and the mutation of these residues in the active site cleft importantly showed a dominant negative effect (20). The expression of PPM1D mutant may interfere with dephosphorylation activity of the endogenous PPM1D and thus function as a dominant negative factor. Thus, the site-specific dephosphorylation of Oct-4 by PPM1D might influence the transcription level.

RA triggers cell differentiation and cell growth inhibition, and it is a promising agent for cancer therapy to induce cell differentiation and cell death (21, 22). I showed that the combined treatment with PPM1D inhibitor and RA facilitates cell differentiation. Our group has also demonstrated that the PPM1D inhibitor supported the effect of doxorubicin in cells that possess C-terminal-truncated PPM1D (23). The PPM1D inhibitor has a potential to enhance the therapeutic effect of RA, as well as anti-cancer agents.

### 3.6. References

1. Lu, X., Nannenga, B., and Donehower, L. A. (2005) PPM1D dephosphorylates Chk1 and p53 and abrogates cell cycle checkpoints. *Genes Dev.* **19**, 1162–1174
2. Cha, H., Lowe, J. M., Li, H., Lee, J. S., Belova, G. I., Bulavin, D. V., and Fornace, A. J. (2010) Wip1 directly dephosphorylates  $\gamma$ -H2AX and attenuates the DNA damage response. *Cancer Res.* **70**, 4112–4122
3. Goloudina, A. R., Kochetkova, E. Y., Pospelova, T. V, and Demidov, O. N. (2016) Wip1 phosphatase: between p53 and MAPK kinases pathways. *Oncotarget.* **7**, 31563–31571
4. Choi, J., Nannenga, B., Demidov, O. N., Dmitry, V., Cooney, A., Brayton, C., Zhang, Y., Mbawuike, I. N., Bradley, A., Appella, E., Donehower, L. a, and Bulavin, D. V (2002) Mice Deficient for the Wild-Type p53-Induced Phosphatase Gene (Wip1) Exhibit Defects in Reproductive Organs, Immune Function, and Cell Cycle Control. *Mol. Cell. Biol.* **22**, 1094–1105
5. Sakai, H., Fujigaki, H., Mazur, S. J., and Appella, E. (2014) Wild-type p53-induced phosphatase 1 (Wip1) forestalls cellular premature senescence at physiological oxygen levels by regulating DNA damage response signaling during DNA replication. *Cell Cycle.* **13**, 1015–1029
6. Zhu, Y. H., Zhang, C. W., Lu, L., Demidov, O. N., Sun, L., Yang, L., Bulavin, D. V., and Xiao, Z. C. (2009) Wip1 regulates the generation of new neural cells in the adult olfactory bulb through p53-dependent cell cycle control. *Stem Cells.* **27**, 1433–1442

7. Le Guezennec, X., Brichkina, A., Huang, Y. F., Kostromina, E., Han, W., and Bulavin, D. V. (2012) Wip1-dependent regulation of autophagy, obesity, and atherosclerosis. *Cell Metab.* **16**, 68–80
8. Zhang, L., Liu, L., He, Z., Li, G., Liu, J., Song, Z., Jin, H., Rudolph, K. L., Yang, H., Mao, Y., Zhang, L., and Zhang, H. (2015) Inhibition of Wild-Type p53-Induced Phosphatase 1 Promotes Liver Regeneration in Mice by Direct Activation of Mammalian Target of Rapamycin. 10.1002/hep.27755
9. Lee, J. S., Lee, M. O., Moon, B. H., Shim, S. H., Fornace, A. J., and Cha, H. J. (2009) Senescent growth arrest in mesenchymal stem cells is bypassed by Wip1-mediated downregulation of intrinsic stress signaling pathways. *Stem Cells.* **27**, 1963–1975
10. Zhu, Y., Demidov, O. N., Goh, A. M., Virshup, D. M., Lane, D. P., and Bulavin, D. V. (2014) Phosphatase WIP1 regulates adult neurogenesis and WNT signaling during aging. *J. Clin. Invest.* **124**, 3263–3273
11. Chuman, Y., Kurihashi, W., Mizukami, Y., Nashimoto, T., Yagi, H., and Sakaguchi, K. (2009) PPM1D430, a novel alternative splicing variant of the human PPM1D, can dephosphorylate p53 and exhibits specific tissue expression. *J. Biochem.* **145**, 1–12
12. Andrews, P. W. (1984) Retinoic acid induces neuronal differentiation of a cloned human embryonal carcinoma cell line in vitro. *Dev. Biol.* **103**, 285–293

13. Deb-Rinker, P., Ly, D., Jezierski, A., Sikorska, M., and Walker, P. R. (2005) Sequential DNA methylation of the Nanog and Oct-4 upstream regions in human NT2 cells during neuronal differentiation. *J. Biol. Chem.* **280**, 6257–6260
14. Ogasawara, S., Kiyota, Y., Chuman, Y., Kowata, A., Yoshimura, F., Tanino, K., Kamada, R., and Sakaguchi, K. (2015) Novel inhibitors targeting PPM1D phosphatase potently suppress cancer cell proliferation. *Bioorganic Med. Chem.* **23**, 6246–6249
15. Sakai, H., Fujigaki, H., Mazur, S., Appella, E., Sakai, H., Fujigaki, H., Mazur, S. J., and Appella, E. (2014) forestalls cellular premature senescence at physiological oxygen levels by regulating DNA damage response signaling during DNA replication forestalls cellular premature senescence at physiological oxygen levels by regulating DNA damage response signaling during DNA replication. 10.4161/cc.27920
16. Chen, Z., Yi, W., Morita, Y., Wang, H., Cong, Y., Liu, J. P., Xiao, Z., Rudolph, K. L., Cheng, T., and Ju, Z. (2015) Wip1 deficiency impairs haematopoietic stem cell function via p53 and mTORC1 pathways. *Nat. Commun.* **6**, 1–11
17. Bae, K. B., Yu, D. H., Lee, K. Y., Yao, K., Ryu, J., Lim, D. Y., Zykova, T. A., Kim, M. O., Bode, A. M., and Dong, Z. (2017) Serine 347 Phosphorylation by JNKs Negatively Regulates OCT4 Protein Stability in Mouse Embryonic Stem Cells. *Stem Cell Reports.* **9**, 2050–2064

18. Spelat, R., Ferro, F., and Curcio, F. (2012) Serine 111 phosphorylation regulates OCT4A protein subcellular distribution and degradation. *J. Biol. Chem.* **287**, 38279–38288
19. Plath, K., Huang, J., Saxe, J. P., Tomilin, A., and Scho, H. R. (2009) Post-Translational Regulation of Oct4 Transcriptional Activity. 10.1371/Citation
20. Dudgeon, C., Shreeram, S., Tanoue, K., Mazur, S. J., Sayadi, A., Robinson, R. C., Appella, E., and Bulavin, D. V. (2013) Genetic variants and mutations of PPM1D control the response to DNA damage. *Cell Cycle.* **12**, 2656–2664
21. Warrell, R. P., Frankel, S. R., Miller, W. H., Scheinberg, D. A., Itri, L. M., Hittelman, W. N., Vyas, R., Andreeff, M., Tafuri, A., Jakubowski, A., Gabilove, J., Gordon, M. S., and Dmitrovsky, E. (1991) Differentiation Therapy of Acute Promyelocytic Leukemia with Tretinoin (All-trans-Retinoic Acid). *N. Engl. J. Med.* **324**, 1385–1393
22. Siddikuzzaman, Guruvayoorappan, C., and Berlin Grace, V. M. (2011) All trans retinoic acid and cancer. *Immunopharmacol. Immunotoxicol.* **33**, 241–249
23. Kozakai, Y., Kamada, R., Kiyota, Y., Yoshimura, F., Tanino, K., and Sakaguchi, K. (2014) Inhibition of C-terminal truncated PPM1D enhances the effect of doxorubicin on cell viability in human colorectal carcinoma cell line. *Bioorganic Med. Chem. Lett.* **24**, 5593–5596



## **4. Regulation of the retinoic signal pathway via dephosphorylation of ERK-1/2**

### **4.1. Abstract**

RA classically exerts activities to regulate gene expression via binding to nuclear RA receptors. Additionally, RA rapidly and transiently induces activation of MAPKs, such as extracellular signal regulated kinase 1/2 (ERK-1/2) and p38 MAPK. However, it remained unclear what kind of protein is involved and how non-classical activity is regulated.

In this study, I found that PPM1D phosphatase is involved in RA-induced ERK regulation. I demonstrated that RA treatment rapidly and transiently induces phosphorylation of ERK-1/2 in NT2/D1 cells. RA acted upstream of MAP kinase/ERK kinase (MEK). PPM1D dephosphorylated a phosphopeptide containing a sequence derived from ERK-1/2 in *in vitro* phosphatase assay. Treatment with the PPM1D inhibitor SL-176 facilitated phosphorylation of ERK-1/2 in NT2/D1 cells. Intriguingly, treatment of ERK inhibitor promoted RA-induced differentiation. These results suggested that PPM1D modulates the phosphorylation level of ERK-1/2 evoked by the RA-MEK-ERK pathway. It is likely that the regulation of ERK-1/2 phosphorylation coordinates appropriate RA-induced cell differentiation.

## 4.2. Introduction

Vitamin A or retinol is an important compound for healthy vision, immune system function, and reproduction. RA is the active metabolite of vitamin A, and RA signaling plays an essential role in embryonic development. In the classical model of RA-induced gene activation, RA binds to the RAR which forms a heterodimer complex with RXR. RA binding induces a conformational change in the RAR-RXR complex and promotes the replacement of co-factors, resulting in RA-mediated gene activation and repression (1). Recent studies have revealed non-classical effects of RA, such as activation of the MAPKs signaling pathway (2). RA treatment activated the p38 MAPK pathway in several cell lines, such as acute promyelocytic leukemia, breast carcinoma, and mouse embryonic fibroblasts (3, 4). The activation of p38 induced activation of the downstream MSK1 and its pathway facilitated RA-targeted gene expression. It was mediated by RARs localized in lipid rafts at the plasma membrane, where it forms complexes with G protein alpha Q (4). RA also rapidly and transiently activated ERK-1/2 (also known as p42/p44 MAPKs) in neuroblastomas, neurons, and embryonic stem cells (5–7). It has been reported that the activation of RARs localized in a lipid membrane and phosphatidylinositol-3-kinase are involved. MAPKs phosphorylate several target proteins, such as MSK1, histones, corepressors, and coactivators. These phosphorylation processes facilitate RA-induced gene expression via effective promotion of the exchange of the co-factors (8).

Section 3 described the lack of significant changes in *POU5F1* levels immediately after RA exposure. However, PPM1D inhibition affected *POU5F1* levels within 12 h after RA treatment. These results prompted me to examine the involvement of PPM1D in the

early phases of RA signaling. In this study, I investigated the role of PPM1D in RA non-classical effects.

### **4.3. Experimental procedures**

#### **4.3.1. Cell lines and materials**

NT2/D1 (NTERA-2 cl. D1) human teratocarcinoma cells were obtained from American type tissue culture collection (ATCC) (Rockville, MD, USA). Rabbit polyclonal anti-PPM1D was prepared as previously described (9). Other antibodies used include: anti-Oct-4 (C-10) (sc-5279) and anti-GAPDH (FL-335) (sc-25778) from Santa Cruz Biotechnology; anti-Phospho-p44/42 MAPK(Thr202/Tyr204) (197G2) (#4377), anti-p44/42 MAPK (#9102), anti-Phospho-p38 MAPK(Thr180/Tyr182) (12F8) (#4631), anti-p38 MAPK (#9212) and anti-rabbit IgG HRP-linked Antibody (7074) from Cell Signaling Technology; and anti-mouse IgG HRP-linked Antibody (NA931) from GE healthcare. PPM1D inhibitor SL-176 was obtained from Laboratory of Organic Chemistry II (Faculty of Science, Hokkaido University). PD0325901 was obtained from AdooQ Bioscience. SCH772984 was obtained from Cayman Chemical.

#### **4.3.2. Cell manipulation**

NT2/D1 cells were cultured in Dulbecco's modified Eagles medium supplemented with 10% v/v fetal bovine serum with 100 µg/ml of streptomycin and 100 units/ml of penicillin at 37 °C in a humidified 5% CO<sub>2</sub> incubator. NT2/D1 cells were plated onto 35 mm dish with 1.5 ml of medium and incubated for 24 h before operation. Cells were treated with RA and inhibitors after 24 h of transfection. Change and refresh medium containing compounds every 2 days.

#### 4.3.3. Western blotting

All cells were rinsed with PBS twice and lysed in 1x sample buffer (50 mM Tris-HCl, pH 6.8, 10% Glycerol, 2% SDS). Cell lysates were normalized for total protein using BCA Protein Assay Kit (Pierce) and then added 2-mercaptoethanol to 6%. Protein were separated by SDS-PAGE and transferred to polyvinylidene difluoride membranes. Proteins were detected by enhanced chemiluminescence with the above antibodies.

#### 4.3.4. *In vitro* phosphatase assay

PPM1D(1-420) was purified as His-tag protein as previously described (10). All peptides were manually synthesized using the Fmoc protection strategy of solid phase peptide synthesis. Fmoc amino acids were obtained from Novabiochem. The peptide fractions were purified manually by reverse-phase HPLC using Vydac C 8 (22x 250 mm). The HPLC peaks were analyzed by MALDI-TOF-MS. Phosphatase activity assays by measuring the released free phosphate using the BIOMOL GREEN Reagent (Enzo life sciences). All assays were carried out by incubation with phosphopeptides (20 and 100  $\mu$ M) and His-PPM1D(1-420) (2 nM) for 3 min at 30 °C. Substrate sequences were Ac-VEPPLS(P)QETFSDLW-NH<sub>2</sub> (p53(pS15)) and Ac-DHTGFLT(P)EY(P)VATR-NH<sub>2</sub> (ERK-1/2 (pT202, pY204))

## 4.4. Results

### 4.4.1. Activation of MEK-ERK-1/2 signaling following RA treatment in NT2/D1 cells

I examined the non-genomic effects of RA in NT2/D1 cells such as phosphorylation of MAPKs. I found that ERK-1/2 were rapidly and transiently phosphorylated in 5 min by treatment with RA (**Figure 4-1**). To confirm the upstream ERK-1/2 phosphorylation following RA treatment, I used the MEK inhibitor PD0325901 and analyzed ERK-1/2 phosphorylation levels. Before RA treatment, NT2/D1 cells were preincubated with PD0325901 for 30 min. PD0325901 treatment impaired the RA-induced phosphorylation of ERK-1/2 (**Figure 4-2**). These results indicated that the MEK/ERK signaling pathway is stimulated by RA treatment.

### 4.4.2. Dephosphorylation of ERK-1/2 peptide in *in vitro* phosphatase assay

ERK-1/2 are phosphorylated with a highly conserved TEY motif (Thr 202 and Tyr 204 in human ERK-1, Thr 185 and Tyr 187 in human ERK-2), and dual phosphorylation is required for full enzyme activation (11). I carried out *in vitro* phosphatase assays using a double phosphorylated peptide TEY to examine whether PPM1D dephosphorylates ERK-1/2 peptide. PPM1D dephosphorylated ERK-1/2(pTEpY) peptide *in vitro* at a level that was approximately equal to phosphatase activity towards p53(pS15), which is a well-known target for PPM1D (**Figure 4-3**).

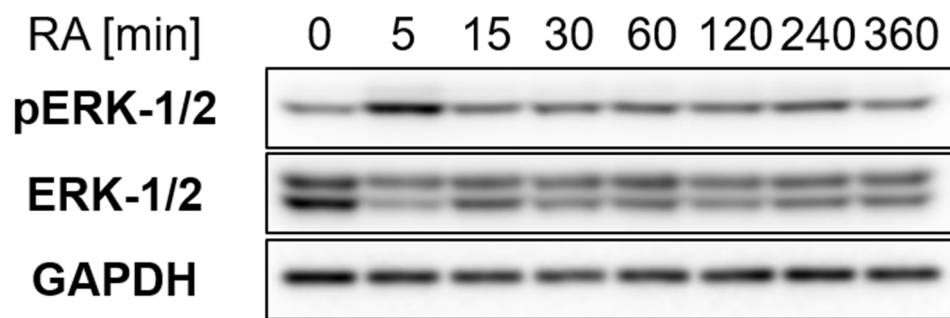


**Figure 4-1.** Effect of RA treatment on rapid MAPKs activation in NT2/D1 cell. NT2/D1 cells were treated with 10  $\mu$ M RA and harvested at the indicated times. Data are representative of three independent experiments.

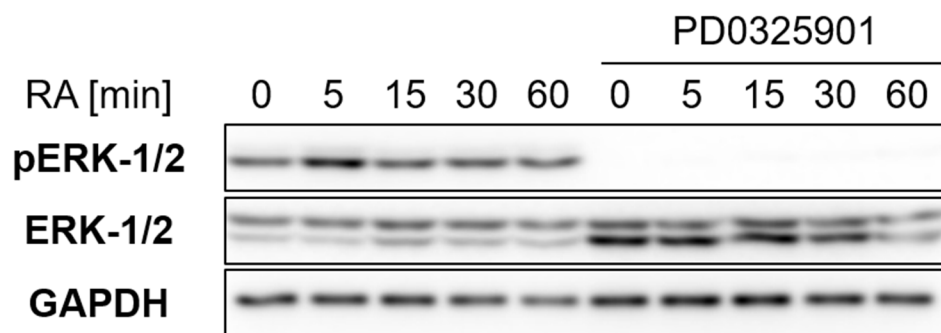


**Figure 4-2.** Activation of MEK-ERK pathway by RA treatment. NT2/D1 cells were pre-incubated with 1  $\mu$ M MEK inhibitor PD09325901 or DMSO for control. After 30 min, the cells were treated with 10  $\mu$ M RA for the indicated times. Data are representative of two independent experiments.



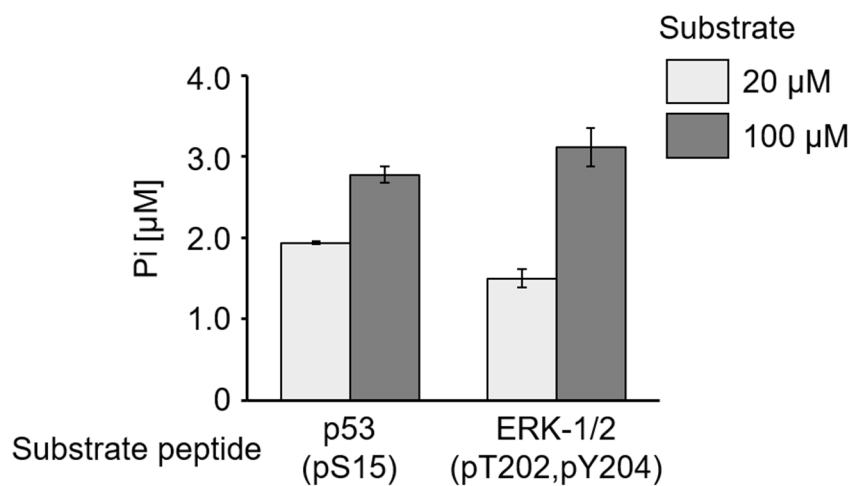


**Figure 4-3.** *In vitro* phosphatase assay toward ERK-1/2(pT202, pY204) peptide. *In vitro* phosphatase assay of His-PPM1D(1-420) (2 nM) towards the indicated phosphopeptides (20 and 100 μM) using BIOMOL GREEN reagent. Value are the mean ± range of duplicates. Data are representative of two independent experiments.

#### **4.4.3. Effect of SL-176 treatment on RA-induced ERK-1/2 activation**

To examine whether PPM1D is involved in ERK-1/2 activation in response to RA treatment, I used the PPM1D inhibitor SL-176 and analyzed the phosphorylation level of ERK-1/2. Combined treatment with SL-176 and RA showed markedly increased phosphorylation of ERK-1/2 (**Figure 4-4**). These data indicated that PPM1D is involved in RA-induced ERK-1/2 activation, including the possibility that PPM1D directly dephosphorylates ERK-1/2 in cells.

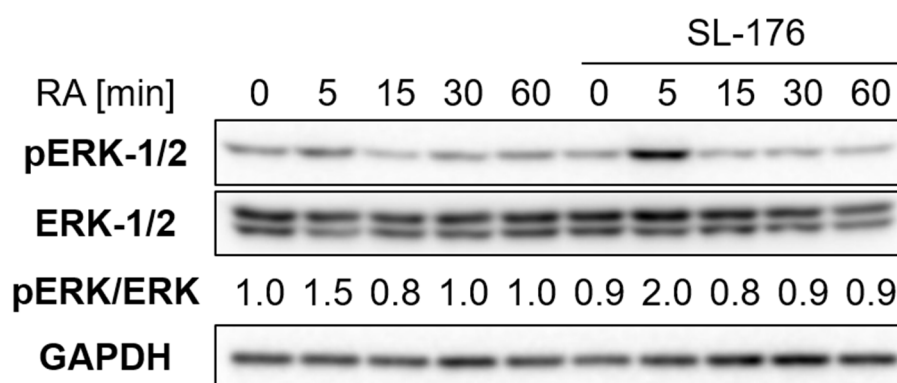


**Figure 4-4.** Effect of SL-176 treatment on ERK-1/2 phosphorylation by RA treatment. NT2/D1 cells were pretreated with 7.5  $\mu$ M SL-176 for 24 h, and cells were treated with 10  $\mu$ M RA for the indicated times. The ratios of signal intensity for pERK/ERK were shown below the panel of western blotting as fold change compared with intensity at time 0. Data are representative of at least three independent experiments.

#### 4.5. Discussion

In this study, I demonstrated that PPM1D mediates the phosphorylation level of ERK-1/2 in RA-induced cell differentiation. I also showed that the activation of ERK-1/2 was evoked by the RA-MEK-ERK pathway. ERK-1/2 signaling generally controls cell proliferation and differentiation. Some studies have shown the activation of p38 MAPK by treatment with RA. The activated MAPK and downstream target genes also appear to depend on the cell type (3, 4). It was previously reported that phosphorylated ERK-1/2 translocates to the nucleus and phosphorylates its target proteins (12, 13). Taken together with my findings, PPM1D modulates and defines the RA signaling threshold via dephosphorylation of ERK-1/2.

Although the phosphorylation levels of ERK linearly increase and decrease in response to stimulation strength, there is a threshold level for ERK activity. In addition, ERK activity shows pulse-like changes, and the pulse frequency, duration, and stimulation interval are also significant factors in the regulation of cell functions (14, 15). For example, persistent ERK activation induced cell differentiation in PC12 cells, whereas transient activation resulted in cell proliferation (16). Therefore, these results suggest that the temporally controlled oscillation change of ERK kinase activity during RA signaling induces cell differentiation. The effect of PPM1D inhibition not only changes the phosphorylation state of ERK but also promotes cell differentiation by disturbing the frequency and timing of signal transmission to downstream proteins. Future studies should clarify the detailed mechanism of oscillation changes and subsequent differentiation states.

#### 4.6. References

1. Cunningham, T. J., and Duester, G. (2015) Mechanisms of retinoic acid signalling and its roles in organ and limb development. *Nat. Rev. Mol. Cell Biol.* **16**, 110–123
2. Al Tanoury, Z., Piskunov, A., and Rochette-Egly, C. (2013) Vitamin A and retinoid signaling: genomic and nongenomic effects. *J. Lipid Res.* **54**, 1761–1775
3. Alsayed, Y., Uddin, S., Mahmud, N., Lekmine, F., Kalvakolanu, D. V., Minucci, S., Bokoch, G., and Plataniias, L. C. (2001) Activation of Rac1 and the p38 Mitogen-activated Protein Kinase Pathway in Response to All-trans-retinoic Acid. *J. Biol. Chem.* **276**, 4012–4019
4. Piskunov, A., and Rochette-Egly, C. (2012) A retinoic acid receptor RAR $\alpha$  pool present in membrane lipid rafts forms complexes with G protein  $\alpha$ Q to activate p38MAPK. *Oncogene.* **31**, 3333–3345
5. Masiá, S., Alvarez, S., de Lera, A. R., and Baretino, D. (2007) Rapid, Nongenomic Actions of Retinoic Acid on Phosphatidylinositol-3-Kinase Signaling Pathway Mediated by the Retinoic Acid Receptor. *Mol. Endocrinol.* **21**, 2391–2402
6. Chen, N., and Napoli, J. L. (2007) All-trans-retinoic acid stimulates translation and induces spine formation in hippocampal neurons through a membrane-associated RAR. *FASEB J.* **22**, 236–245

7. Persaud, S. D., Lin, Y. W., Wu, C. Y., Kagechika, H., and Wei, L. N. (2013) Cellular retinoic acid binding protein I mediates rapid non-canonical activation of ERK1/2 by all-trans retinoic acid. *Cell. Signal.* **25**, 19–25
8. Rochette-Egly, C. (2015) Retinoic acid signaling and mouse embryonic stem cell differentiation: Cross talk between genomic and non-genomic effects of RA. *Biochim. Biophys. Acta - Mol. Cell Biol. Lipids.* **1851**, 66–75
9. Chuman, Y., Kurihashi, W., Mizukami, Y., Nashimoto, T., Yagi, H., and Sakaguchi, K. (2009) PPM1D430, a novel alternative splicing variant of the human PPM1D, can dephosphorylate p53 and exhibits specific tissue expression. *J. Biochem.* **145**, 1–12
10. Ogasawara, S., Kiyota, Y., Chuman, Y., Kowata, A., Yoshimura, F., Tanino, K., Kamada, R., and Sakaguchi, K. (2015) Novel inhibitors targeting PPM1D phosphatase potently suppress cancer cell proliferation. *Bioorganic Med. Chem.* **23**, 6246–6249
11. Zhou, B., and Zhang, Z. Y. (2002) The activity of the extracellular signal-regulated kinase 2 is regulated by differential phosphorylation in the activation loop. *J. Biol. Chem.* **277**, 13889–13899
12. Adachi, M., Fukuda, M., and Nishida, E. (2000) Nuclear export of MAP kinase (ERK) involves a MAP kinase kinase (MEK)-dependent active transport mechanism. *J. Cell Biol.* **148**, 849–56

13. Brami-Cherrier, K., Roze, E., Girault, J. A., Betuing, S., and Caboche, J. (2009) Role of the ERK/MSK1 signalling pathway in chromatin remodelling and brain responses to drugs of abuse. *J. Neurochem.* **108**, 1323–1335
14. Aoki, K., Kumagai, Y., Sakurai, A., Komatsu, N., Fujita, Y., Shionyu, C., and Matsuda, M. (2013) Stochastic ERK activation induced by noise and cell-to-cell propagation regulates cell density-dependent proliferation. *Mol. Cell.* **52**, 529–540
15. Shindo, Y., Iwamoto, K., Mouri, K., Hibino, K., Tomita, M., Kosako, H., Sako, Y., and Takahashi, K. (2016) Conversion of graded phosphorylation into switch-like nuclear translocation via autoregulatory mechanisms in ERK signalling. *Nat. Commun.* **7**, 1–10
16. Traverse, S., Seedorf, K., Paterson, H., Marshall, C. J., Cohen, P., and Ullrich, A. (1994) EGF triggers neuronal differentiation of PC12 cells that overexpress the EGF receptor. *Curr. Biol.* **4**, 694–701

## 5. Conclusions

The protein phosphatase PPM1D is an important factor for normal homeostasis and pathogenesis of several diseases. PPM1D dephosphorylates various critical factors and negatively regulates the p53 pathway and DNA damage checkpoints. Gene amplification of *PPM1D* and protein overexpression occurred in tumors. Recent studies revealed the physiological functions of PPM1D in neurogenesis, immunity, and maintenance of stemness. Cell differentiation is properly regulated by intrinsic and extrinsic signaling pathways. However, many signaling cascades that control cell differentiation are still incompletely understood. Many substrates of PPM1D are involved in several intracellular signaling pathways that regulate both pluripotency and cell differentiation. Therefore, it is important to investigate the function of PPM1D in cell differentiation. In this study, I showed the function of PPM1D as a negative regulator in the RA signaling pathway. I also developed PPM1D inhibitors to increase the inhibitory activity of PPM1D.

In section 2, I described SAR studies to characterize and improve the inhibitory activity of SL-176. Substitution of two hydrophobic moieties to hydrogen decreased inhibitory activity against PPM1D. This study showed that sterically demanding hydrophobic groups, but not planar hydrophobic groups, are suited as SL-176 analogs to inhibit PPM1D activity. A primary alcohol SL-175 had potent inhibition of phosphatase activity *in vitro*, while SL-175 showed moderate inhibition of cell viability. An amine form, SL-177, had low inhibition for PPM1D, while SL-177 strongly suppressed cell viability. Amino alkyl-ester compounds, SL-180 and SL-183, potently inhibited cell



viability, more so than SL-176. A fluorescein with 4-aminobutyl-ester was incorporated into cells faster than a fluorescein with carboxyl acid. SL-183 specifically suppressed the viability of PPM1D-overexpressed cells. These results indicated that the introduction of an amine or amino alkyl-ester band into SL-176 improves inhibitory activity against PPM1D.

In section 3, I examined the role of PPM1D in RA-induced cell differentiation. I showed that PPM1D knockdown induced differentiation in NT2/D1 cells. Treatment with SL-176 also reduced the expression level of Oct-4. SL-176 facilitated RA-induced cell differentiation in terms of decreasing of *POU5F1* mRNA level. Moreover, inactivated PPM1D enhanced RA-induced cell differentiation. These results suggested that PPM1D is essential for maintaining an undifferentiated state and PPM1D activity affected RA-induced cell differentiation.

In section 4, I investigated the effect of PPM1D on non-genomic effects of RA. Treatment with RA rapidly and transiently induced activation of the MEK-ERK pathway. PPM1D dephosphorylated ERK-1/2 and treatment with SL-176 facilitated the phosphorylation of ERK-1/2 evoked by RA treatment. It is likely that the regulation of ERK-1/2 phosphorylation coordinates appropriate RA-induced cell differentiation. These results suggested that PPM1D modulates non-classical effects of RA via dephosphorylation of ERK-1/2.

In summary, I have reported novel PPM1D inhibitors by SAR studies of SL-176 against the oncogene PPM1D. I also identified new targets and regulatory pathways of PPM1D in cell differentiation. These studies provide valuable inhibitors for cancer

therapy and for elucidation of carcinogenesis mechanisms, and contribute to clarifying the mechanism of signal transduction that controls cell differentiation.

## 6. Acknowledgement

I would like to express my appreciation to my supervisor Professor Kazuyasu Sakaguchi (Laboratory of Biological Chemistry) for the continuous support of my study and related research, and extensive discussion.

I would like to thank Professor Yota Murakami (Laboratory of Bioorganic Chemistry), Professor Mutsumi Takagi (Laboratory of Cell Processing Engineering), Professor Keiji Tanino (Laboratory of Organic Chemistry II) and Associate Professor Toshiaki Imagawa (Laboratory of Biological Chemistry) for their valuable comments and discussions on my thesis.

My sincere gratitude also goes to the collaborators of this work, Professor Keiji Tanino, Mr. Ryusei Ito (Laboratory of Organic Chemistry II), Mr. Shoya Tanaka (Laboratory of Organic Chemistry II) and Dr. Fumihiko Yoshimura (University of Shizuoka) who provided valuable inhibitors and guidance on my studies. I am also immensely grateful to Ms. Seiko Oka (Global Facility Center, Hokkaido University) for the LC-MS/MS measurements.

I wish to express my appreciation to Dr. Toshiaki Imagawa and Dr. Yoshiro Chuman (Niigata University) who provide helpful comments and support not only for technical help. I also wish to thank Assistant Professor Rui Kamada for her tremendous support on writing papers. I am very grateful to all the members of the Laboratory of Biological Chemistry.

Finally, I would like to thank my family for the continuous support and encouragement throughout my studies and my life in general.